

Energy efficient retrofitting of buildings in Brazil

Final Report

of the cooperative research project between

HafenCity University (HCU, Hamburg, Germany)

State University of Campinas (Unicamp, Campinas, Brazil)

As a part of the Novas Parcerias (NoPa II) program funded by

German Academic Exchange Service (DAAD)

Coordenação de Aperfeiçoamento de Pessoal de Nível Superior (CAPES)

February, 8th 2018



HafenCity University Hamburg

Facade Systems and Building Envelopes

Prof. Dr.-Ing. Frank Wellershoff

Überseeallee 16

D-20457 Hamburg

Germany



State University of Campinas

Laboratório de Conforto Ambiental

e Física Aplicada (LaCAF)

Profª. Dra. Lucila Chebel Labaki

Cidade Universitária Zeferino Vaz

Barão Geraldo, Campinas – SP, 13083-970

Brazil

Project Team

HafenCity University (HCU)

M.Sc. Matthias Friedrich
M.Eng. Klaus Schweers
Prof. Dr.-Ing. Frank Wellershoff

Professorship for
Facade Systems and Building Envelopes

Überseealle 16
D-20457 Hamburg
Germany

Project Team

State University of Campinas (Unicamp)

Dra. Luciana Fernandes
M.Sc. Beatriz Arantes
Profa. Dra. Lucila Chebel Labaki

Laboratório de Conforto Ambiental
e Física Aplicada (LaCAF)

Cidade Universitária Zeferino Vaz
Barão Geraldo, Campinas – SP, 13083-970
Brazil

Partners

MGM Produtos Siderúrgicos Ltda.
Av. Atílio Belato, 270
Monsenhor Paulo - Minas Gerais
Brazil



Christophe Lenderoth GmbH
Hohweg 5
D-28219 Bremen
Germany



Abstract

Natural ventilation in buildings is a beneficial passive strategy for conditioning buildings for different climates. Beside its potential to promote energy efficiency it can improve indoor air quality in buildings along with health and well-being for their occupants. The achievement of these benefits is related to a good architectural design where type, geometry and location of openings are defined. Different types of openings provide different air change rates. A parameter to distinguish windows regarding their ventilation efficiency is the discharge coefficient. It describes the actual airflow in relation to the ideal airflow. The discharge coefficient varies according to the type of opening, ventilation area besides other physics factors as pressure, velocity and air density. Recent researches on the topic have used the same value of discharge coefficient for different window types. This simplification implies inaccurate results in the estimation of airflow provided by the openings. More reliable values based on experimental analysis can be found in the literature for some types of openings. In order to complement these studies this research aims to characterize additional window types produced in Brazil and Germany. Wind tunnel measurements are performed at the *State University of Campinas* (Unicamp).

With measured discharge coefficients thermal building simulations are done for a typical office room in Brazil. It is found that the use of double glazing halves the energy demand for cooling. A simple control algorithm for air conditioning is developed. In comparison with a usually used constant setpoint for air conditioning units the energy demand for cooling can be reduced up to 93%.

Additional tracer gas measurements for direct measurement of the air change rate are done in an office room at the *HafenCity University* (HCU) are done. A strong dependency between wind flow direction and air exchange rate is proved.

Content

1	GOALS	1
2	WIND TUNNEL MEASUREMENTS	2
2.1	AIMS	2
2.2	METHOD	2
2.3	EXPERIMENTAL SETUP	2
2.4	PRESSURE MEASUREMENTS	6
2.5	VELOCITY MEASUREMENTS	7
2.6	VELOCITY ANALYSIS	8
2.7	DETERMINATION OF DISCHARGE COEFFICIENTS	11
3	DETERMINATION OF AIR CHANGE RATE BY USING TRACER GAS	15
3.1	AIMS	15
3.2	COMPARISON OF DIFFERENT TRACER GASES	16
3.2.1	<i>Desired properties of the tracer gas</i>	<i>16</i>
3.2.2	<i>Carbon dioxide (CO₂)</i>	<i>16</i>
3.2.3	<i>Sulfur hexafluoride (SF₆)</i>	<i>17</i>
3.2.4	<i>Nitrous oxide (N₂O), Hexafluorobenzene (C₆F₆) and other tracer gases</i>	<i>17</i>
3.3	MATHEMATICAL BACKGROUND	17
3.4	ERROR ANALYSIS	18
3.5	TRACER GAS PROCEDURES	18
3.5.1	<i>Concentration decay method</i>	<i>18</i>
3.5.2	<i>Constant emission method</i>	<i>19</i>
3.5.3	<i>Constant concentration method</i>	<i>20</i>
3.6	EXPERIMENTAL SETUP AND REQUIREMENTS FOR THE MEASUREMENT	21
3.7	WEATHER CONDITIONS	22
3.8	RESULTS	24
3.9	CONCLUSION	26
4	COMPUTER MODELING AND RESULTS ANALYSIS	27
4.1	METHODS	27
4.2	BUILDING DESCRIPTION	27
4.3	ENERGYPLUS AND MATLAB Co-SIMULATION	28
4.4	PARAMETER STUDY	30
4.5	INFLUENCE OF TIMESTEP	34
4.6	GLAZING TYPE	36
4.7	RESULTS	37
4.7.1	<i>Influence of permanent ventilation</i>	<i>37</i>
4.7.2	<i>Influence of shading</i>	<i>38</i>
4.7.3	<i>Influence of glazing type</i>	<i>39</i>
4.7.4	<i>Influence of air conditioning setpoints</i>	<i>40</i>

4.7.5	<i>Design recommendations</i>	41
4.8	CONCLUSION	45
5	KNOWLEDGE TRANSFER	46
5.1	SBE16 - INTERNATIONAL CONFERENCE ON SUSTAINABLE BUILT ENVIRONMENT (SBE)	46
5.2	TRAINING SCHOOL – ADAPTIVE FACADES 2016 (HAMBURG, GERMANY).....	46
5.3	WORKSHOP “RESEARCH INTO USE”	48
5.4	TRAINING SCHOOL – DESIGN PROCESS FOR BUILDING RETROFIT 2017 (CAMPINAS, BRAZIL)	49
6	ACKNOWLEDGEMENTS	50

1 Goals

The aim of this project is to develop an architectural procedure for building retrofit focusing on the use of natural ventilation. Natural ventilation is a passive strategy for cooling that also provides better indoor air quality in workplaces and dwellings. The study is applied in different climates with computer models developed from the data obtained in the experimental measurements.

Experimental measurements are done with the window samples from Brazil and Germany in the wind tunnel at *Unicamp*. Tracer gas measurements are done in an office room at *HCU*. The aim of these measurements is to obtain the discharge coefficient of the windows. The parameter is used as input for the computational models. The computer simulation allows making quantitative analysis of the airflow through the windows and the resulting room comfort.

The results obtained with computer simulations base the development of design recommendations for sizing openings to simplify future projects with natural ventilation. The results are presented in graphs to be used by designers.

2 Wind tunnel measurements

2.1 Aims

The investigation of the properties of openings for natural ventilation is the current subject of many researches around the world by using different approaches. The discharge coefficient c_D is one among other parameters that has significant influence on airflow estimation. It describes the actual airflow in relation to the ideal airflow. The discharge coefficient varies according to the type of opening, ventilation area besides other physics factors as pressure, velocity and air density. The prediction of c_D is being widely done by numerical models using a constant value for different types of windows, what is known from recent research [1] [2] to be a wrong assumption. The estimation of c_D for an opening is neither an easy nor cheap task. The aim of this research is to validate a method for estimating the c_D of full-scale windows by wind tunnel measurements and thus contributing with unknown data of discharge coefficients.

2.2 Method

According to a review done by Chen [3], full- and small-scale models have been used to validate analytical, empirical or numerical models and both are subject to approximations of boundary conditions and flow geometry. Even though, full-scale models have been widely used for predicting ventilation performance in buildings because they give the most realistic predictions.

For avoiding scaling errors due to complex geometry of the windows the measurements are done directly in the real windows installed on the inlet of a wind-tunnel described below.

2.3 Experimental setup

The method in this research is based on the British Standard BS EN 13141-1:2004 [4]. The standard gives recommendations on measuring volume flow rate through openings. The thickness of the board where the windows are mounted is 15 mm, rigid enough to avoid pulsing airflow but not as thick as a wall to not interfere on the measurements. The sensors of pressure of the wind tunnel provide a maximum pressure difference of 1 kPa (in accordance with the British Standard which recommends a range from 0 Pa to 100 Pa). The distance between inlet and outlet is longer than 0.5 m and the distances between the edges of the board and the edges of the openings are larger than 0.3 m. In order to minimize the uncertainties of the results using scaled models, the window samples are fixed at the air inlet of the wind tunnel (Figure 1).

The experiment is carried out in the wind-tunnel of the Laboratory of Environmental Comfort and Applied Physics at the School of Civil Engineering, Architecture and Urban Design at *Unicamp*. It is a linear open-circuit wind-tunnel of 9.03 m length with a test section of 4.80 m length and

0.72 m² transversal area. When the tunnel is not obstructed the assembly motor-fan with power of 12.5 HP provides maximum air velocity of 20 m/s (at 850 rpm). The transversal section is reduced about six times from the inlet (4.20 m²) for reducing the turbulence and the flow to become laminar. The upper part of the test section is adjustable to equalize the static pressure along it. Finally, the air passes through a diffuser of 1.25 m diameter.

The windows installed in the inlet of the tunnel are illustrated in Table 1. Beside the window samples, the boards where the windows are installed are also tested with orifices of 40 x 40 cm and 120 x 100 cm.

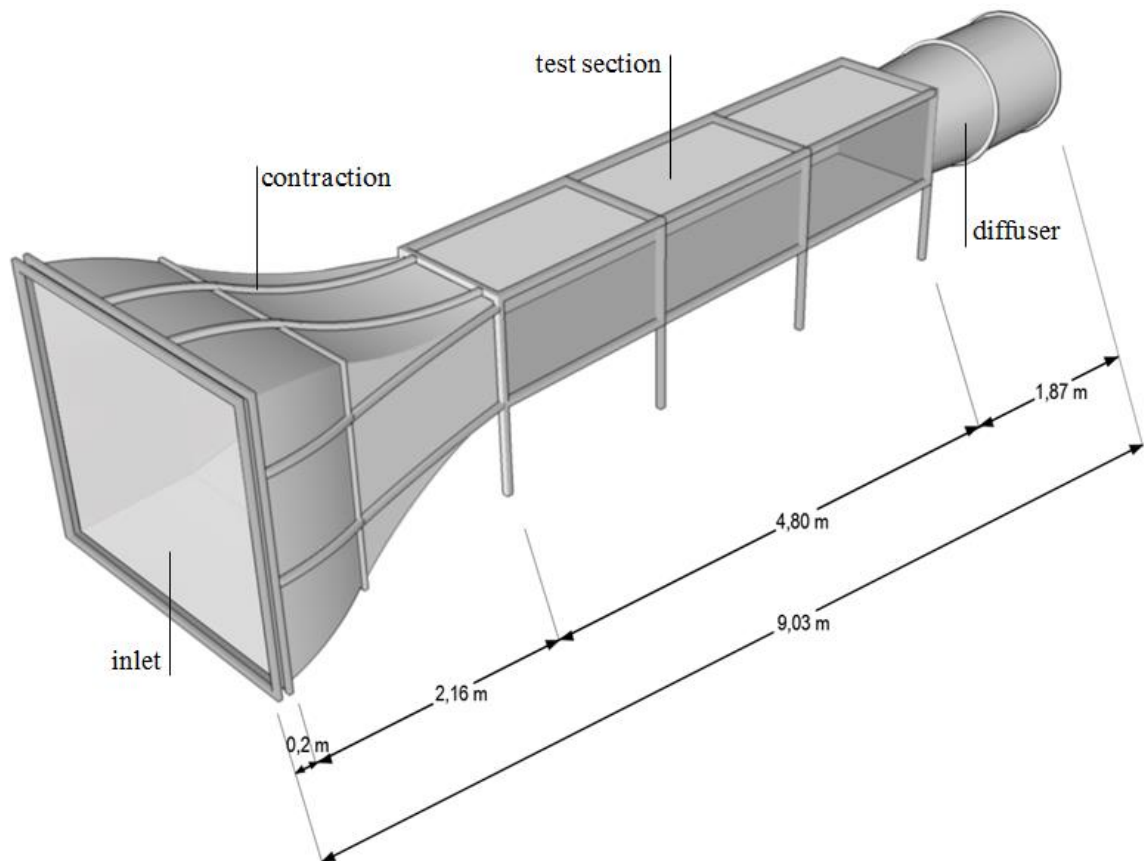


Figure 1: Components of the wind tunnel and their dimensions

Table 1: Window samples installed in front of the wind tunnel inlet











 <p><i>Maxim-ar 45°</i> (awning window, tilted outside)</p>	 <p><i>Maxim-ar 90°</i> (awning window, tilted outside)</p>	 <p><i>Boca de Lobo Fixo</i> (two parallel panes, permanent open, gap in between)</p>	 <p><i>Veneziana Flaps</i> (closed) (Sliding panels with adjustable flaps)</p>
 <p><i>Veneziana Flaps</i> (open) (Sliding panels with adjustable flaps)</p>	 <p><i>Veneziana Holes</i> (closed) (Sliding panels with holes) detailed in Figure 2</p>	 <p><i>Veneziana Holes</i> (open) (Sliding panels with holes)</p>	 <p><i>Dreh-Kipp-Fenster</i> (Bottom hung inside-tilted window)</p>
 <p><i>Parallelausstell- fenster</i> (parallel opening)</p>	 <p><i>Dachfenster</i> (Top hung outside-tilted window)</p>	 <p><i>Orifice 40x40 cm</i> (rectangular opening without a window)</p>	 <p><i>Orifice 120x100 cm</i> (rectangular opening without a window)</p>



Figure 2: Veneziana Holes in detail

The wind tunnel is equipped with pressure taps and velocity sensors to calculate the discharge coefficient described by Equation (2.1) known as *orifice equation*. Explanation on the arrangement of the sensors is given in sections 2.4 and 2.5.

$$c_D = \frac{Q}{A} \sqrt{\frac{\rho}{2\Delta P}} \quad (2.1)$$

Where:

- c_D : discharge coefficient [-]
- Q : airflow [m^3/s]
- A : opening area [m^2]
- ρ : air density [kg/m^3]
- ΔP : difference of pressure [Pa]

It is still an open question within the scientific community whether the orifice equation is accurate for calculating wind-induced flow through openings. Nonetheless, no other proposed formulation appeared to be appropriate to replace the orifice equation [1].

In the present experiment the wind tunnel is sucking the air through the windows. This method may create an airflow coming from different directions (see Figure 3). It is known that the angle of wind incidence is one among other factors that influences the discharge coefficient. This fact, together with the geometry of the windows, may result in different values resulting from the wind tunnel experiments comparing to values from the literature.

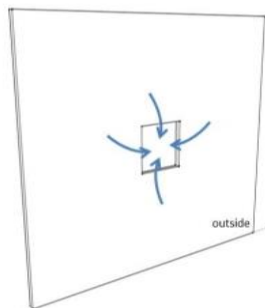


Figure 3: Schematic drawing explaining the airflow in the inlet area of the board containing the windows

2.4 Pressure measurements

The difference of pressure is measured by taps around the window flush to the outside face of the board containing the window and at the inside face of the wind tunnel (Figure 5). Similar setup is described in the work of Chu et al. [5]. Chiu and Etheridge suggest in [6] that the pressure taps should be placed far enough from the opening so the flow through the opening does not influence the pressure but close enough to minimize the effect of non-uniformity in the pressure field.

The external pressure taps are uniformly distributed following the same pattern in all measurements: 10 cm away from the edges of the windows and between each other (Figure 4). The total number of pressure taps around each window is presented in Table 2. The internal pressure taps are installed on the surfaces of the contraction area of the wind tunnel (Figure 6). They are located 20 cm behind the board in the mid-height of the vertical surfaces and in the mid-width of the horizontal surface.

The tests are carried out by continuously increasing pressure difference: from 0 rpm to 600 rpm, recording the data at intervals of 100 rpm. The resulting difference was automatically calculated by the software.

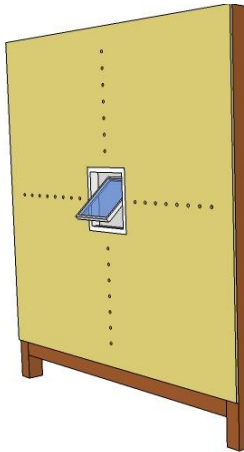


Figure 4: Schematics of the pressure taps distribution around the opening for Maxim-ar 45°



Figure 5: Board with a window sample and pressure taps on the left

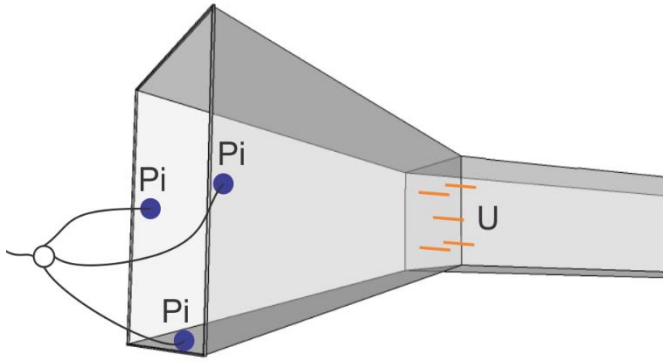


Figure 6: Schematics of the pressure taps and velocity sensors inside the wind tunnel

Table 2: Number of pressure taps around windows

Window type	Number of external pressure taps
Orifice 40x40 cm	30
Orifice 120x100 cm	16
Maxim-ar 45°/90°	30
Boca de Lobo Fixo	30
Veneziana Flaps (open/close)	16
Veneziana Holes (open/close)	16
Dreh-Kipp-Fenster	18
Parallelausstellfenster	18
Dachfenster	18

2.5 Velocity measurements

It is assumed that the airflow becomes linear when entering the test section due to the contraction area. Therefore, five velocity sensors (hot-wire anemometers) are uniformly distributed across the section according to Figure 7. The sensors at the edge are 22 cm apart from the walls and 20 cm from the ceiling and the floor of the test section. The central sensor is in the geometric center of the cross-section.



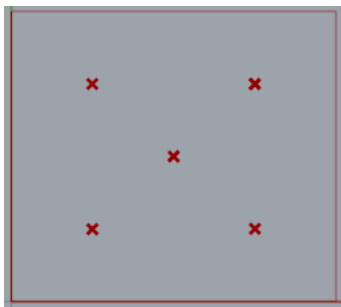
Figure 7: Velocity sensors in the wind tunnel

2.6 Velocity analysis

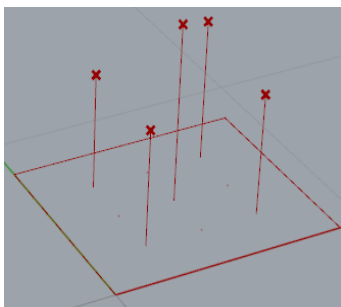
The velocity profile in the wind tunnel cross section is highly influenced by the opening installed in front of the tunnel. Nevertheless, a flow profile is formed where the following assumptions can be made:

- The velocity at the wind tunnel surface is zero,
- The inviscid flow region does not exist due to the influence of the opening,
- The behavior of the velocity distribution is parabolic with the maximum value in the center of the tunnel cross section if not disturbed by an asymmetrically opening.

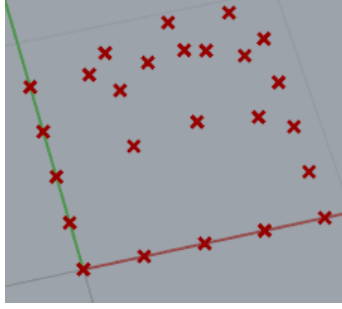
Taking these assumptions into account a graphical analyzing method is developed by using Rhino3d/Grasshopper® software. In order to calculate the discharge coefficient using the orifice equation (Equation (2.1)) the airflow Q is needed.



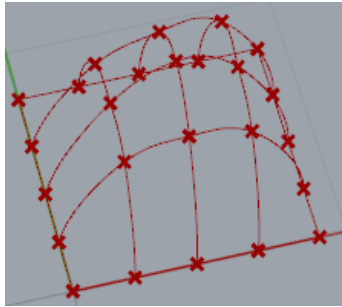
The airflow can be obtained when the flow pattern is known. The measurement of an exact flow pattern is difficult in terms of the number of velocity sensors installed: The higher number of sensors in the cross section allows a higher resolution of flow pattern but also leads to a flow obstacle at the same time. Here, air velocity is measured at five points in the tunnel cross section behind the window.



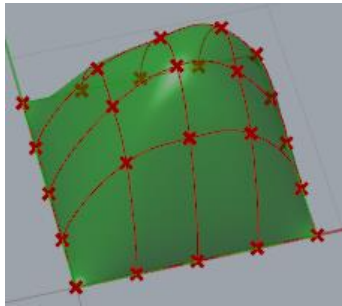
The five measured values of velocity for each type of window are drawn as the height above wind tunnel cross section. The rectangle around represents the surface of the wind tunnel where the velocity is obviously zero. Hence, the picture at the left shows the data which are definitely known. For analyzing the airflow adequately additional data are obtained by interpolation and graphical analysis.



A grid of 5x5 points is created across the wind tunnel section resulting in 16 points at the tunnel surface represent a zero-velocity; five values of velocity measured and the remaining four are interpolated from the data. This grid is used for further analysis. Again, a higher amount of interpolated data would lead to a higher resolution of the flow pattern but it would also increase the uncertainty as the share of known values would decrease.



The points next to each other are connected with an interpolated curve. Two sets of five curves (including the zero-velocity at the wind tunnel surface), one for each u and v direction, are created. It is taken care that the curve behavior corresponds to the expected flow pattern. The huge selection of methods for interpolating data holds the risk of unrealistic values for interpolated velocities.

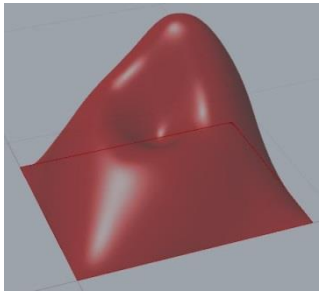
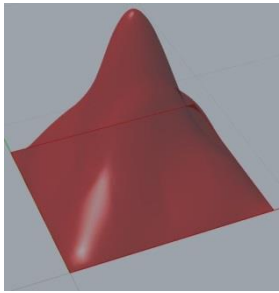
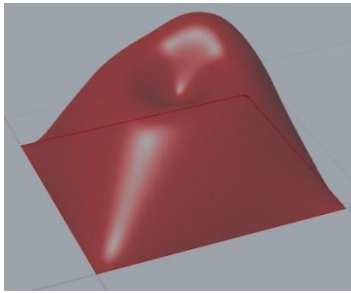
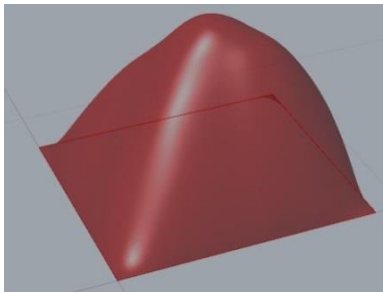
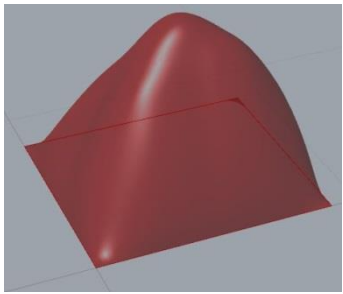
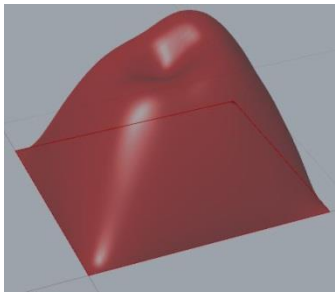
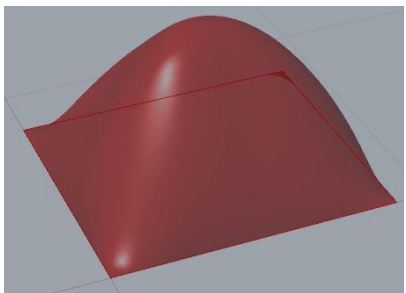
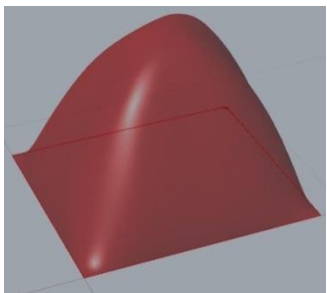
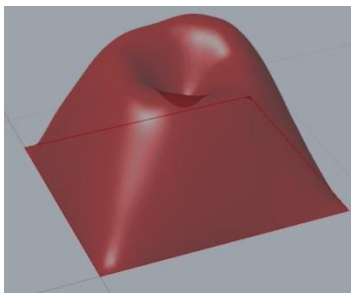
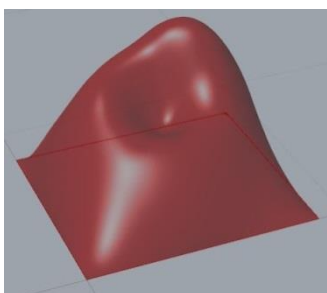
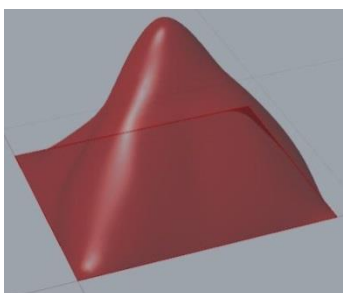
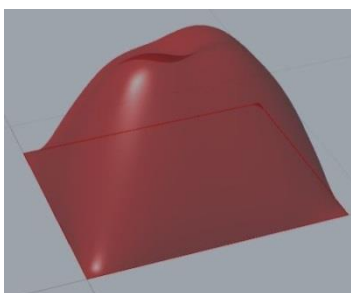


Finally, a differentiable surface is created. This surface describes the best approach of velocity distribution across the wind tunnel. The height of each point on this surface represents the velocity at this point in the wind tunnel.

The airflow $Q = vA$ is defined by the volume below the velocity surface.

Table 3 shows the different flow pattern for the tested window types (not scaled). It can be seen how the geometry and the opening mechanism influences the velocity distribution behind the window. For all windows, the top of the picture is also the top of the wind tunnel cross section. Tilted windows (for example maxim ar-45° and Dachfenster) are characterized by a significantly higher velocity in the upper part of the wind tunnel because the air is channeled by the tilted pane. In case of the Parallelausstellfenster, the air streams almost equally around the pane at all four window sides. Consequently, the velocity sensor in the center of the wind tunnel gives the lowest velocity compared to the four sensors located around.

Table 3: Visualization of flow pattern for all window types

		
Maxim-ar 45°	Maxim-ar 90°	Boca de Lobo Fixo
		
Veneziana Flaps (closed)	Veneziana Flaps (open)	Veneziana Holes (closed)
		
Veneziana Holes (open)	Dreh-KippFenster	Parallelausstellfenster
		
Dachfenster	Orifice 40 x 40 cm	Orifice 120 x 100 cm

2.7 Determination of discharge coefficients

Discharge coefficients are calculated with measured pressure differences and determined airflow by using the orifice equation (see Table 4).

Table 4: Measured values for airflow and pressure difference and c_D -calculations

$c_D = \frac{Q}{A} \sqrt{\frac{\rho}{2\Delta P}}$ <p>ρ = density of air (1.204 kg/m³)</p>				
Window type	Q [m ³ /s]	A [m ²]	ΔP [Pa]	c_D [-]
Orifice 40 x 40cm	3.283	0.16	283.4	0.946
Orifice 120 x 100 cm	7.884	1.20	101.1	0.507
Maxim-ar 45°	2.105	0.16	311.5	0.578
Maxim-ar 90°	2.765	0.16	345.4	0.721
Boca de Lobo Fixo	0.634	0.16	283.2	0.183
Veneziana Flaps (closed)	2.102	1.20	299.4	0.079
Veneziana Faps (open)	5.717	1.20	265.9	0.226
Veneziana Holes (closed)	0.513	1.20	261.3	0.021
Veneziana Holes (open)	6.369	1.20	376.1	0.212
Dreh-Kipp-Fenster	1.932	1.00	198.0	0.107
Parallelausstellfenster	4.025	1.00	300.9	0.180
Dachfenster	2.420	1.00	274.9	0.113

Table 5: Comparison between obtained results and literature references

Company	Window Type	Measured c_D	Literature c_D
-	Orifice 40 x 40 cm ¹	0.946	0.61 [7] 0.80 [8]
	Orifice 120 x 100 cm ²	0.507	0.61 [7]
MGM	Maxim-ar 45°	0.578	0.447 [7] 0.57 [9]
	Maxim-ar 90°	0.721	0.707 [7]
	Boca de Lobo Fixo	0.183	not found
	Veneziana Flaps (closed)	0.079	not found
	Veneziana Flaps (open)	0.026	not found
	Veneziana Holes (closed)	0.021	not found
	Veneziana Holes (open)	0.212	not found
Lenderoth	Dreh-Kipp-Fenster	0.107	0.255 [7]
	Parallelausstellfenster	0.180	not found
	Dachfenster	0.113	0.25 [7]

The discharge coefficient found for the orifice 40x40cm is close to the one found by Ohba et al. [8] in a wind tunnel experiment within similar conditions to this experimental setup. It is also similar to values reported by Sawachi [10] (as shown in Figure 6), if considered that the opening is under the influence of airflow from different directions, as a result of the suction of the fan.

¹ Corresponds to a porosity (total window area divided by the board area) of 4%

² Corresponds to a porosity of 29%

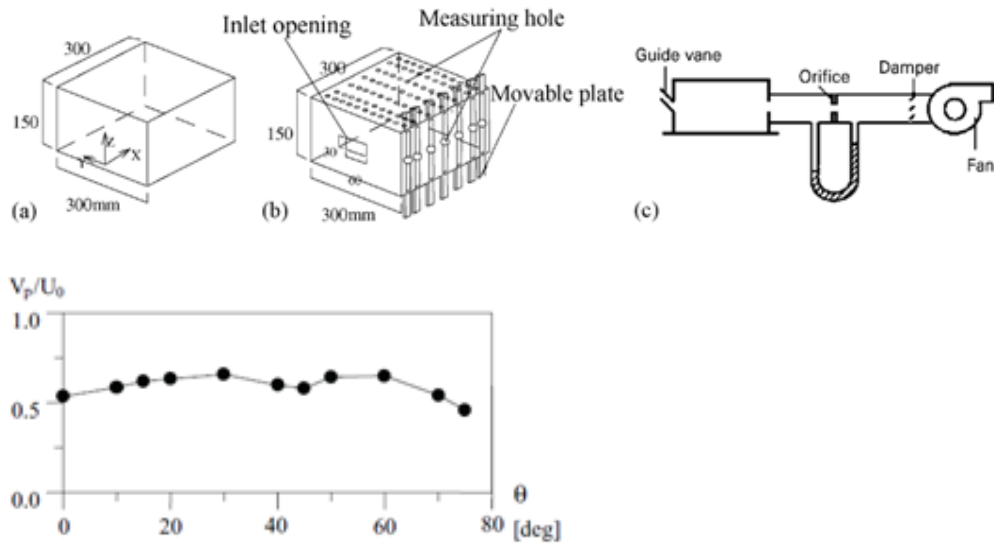


Figure 8: Experimental set up and discharge coefficients found by Ohba et al. [8]

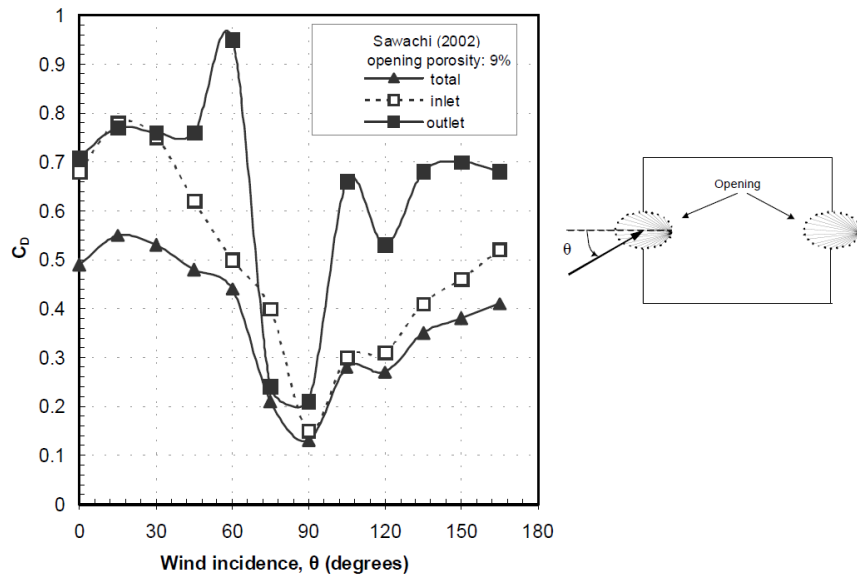


Figure 9: c_D values reported by Sawachi [10]

The discharge coefficient calculated for orifice 120x100cm is close to the reference value provided by Idelchik [7]. Nonstandard values for rectangular openings were also found by Vickery and Karakatsanis [11] and Karava [1]. The authors conducted tests in a boundary layer wind tunnel at 9.1 m/s and measured inlet c_D varying from 0.62 to 0.8.

The reference discharge coefficients for Maxim-ar windows are calculated from the resistance coefficients of a center pivoted window (Figure 10). It should be mentioned, that Maxim-ar windows are not center pivoted. For 45° this value gives a good approximation. For 90° the pivot point is in the center.

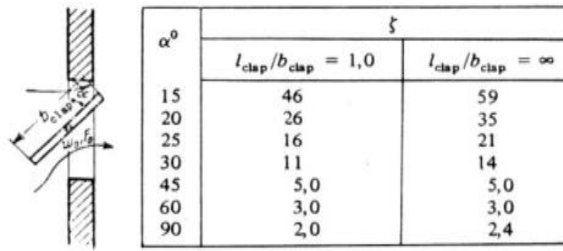


Figure 10: Resistance coefficients for center pivoted windows [7]

$$c_D = \frac{1}{\sqrt{\zeta}} \quad (2.1)$$

The discharge coefficient of the Dreh-Kipp-Fenster is compared to an exhaust, single top-hinged flap [7]. The resistance coefficient value reported by the author and used for calculating the c_D of the referred window is shown in Figure 11. The window installed has an opening angle of 7.6° which is out of the range of reported values. By extrapolation using curve fitting a resistance coefficient of 15.4 respectively $c_D = 0.255$ is found.

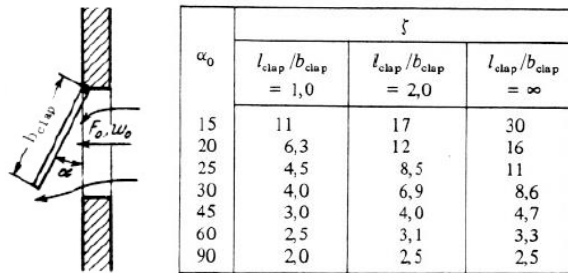


Figure 11: Resistance coefficients for exhale top-hinged flaps [7]

The calculated discharge coefficient of the Dachfenster is compared with an inhale, single top-hinged flap [7] as shown in Figure 12.

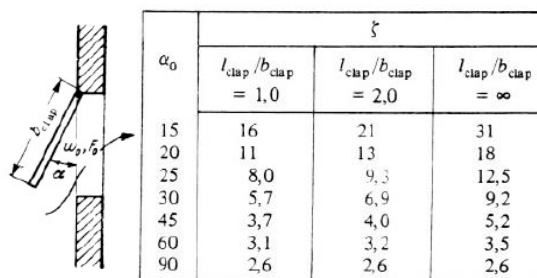


Figure 12: Resistance coefficients for inhale top-hinged flaps [7]

It is intended to proceed to new measurements to confirm the results. This study demands further investigations to understand the resulting airflow in the inlet and outlet areas close to the windows, besides the characteristics of the openings for single-sided ventilation, buoyancy situations and different incidence angle of wind. It is also necessary to take into account unresolved questions as the applicability of the orifice equation. Tracer gas measurements and experiment setups which allow the measurement of the airflow through the openings may be used for these purposes.

3 Determination of air change rate by using tracer gas

3.1 Aims

The measurement of air change rates in buildings is a difficult task. The tracer gas method is a reliable method for this. However, interpretation of results is not straightforward. In occupied rooms additional requirements are made for the use of tracer gas in order to avoid health hazards and to reduce the impact on the environment.

In this project repetitive measurements of air change rate in one office room at the *HCU* with two bottom-hung tilted windows (see Figure 13) are made.

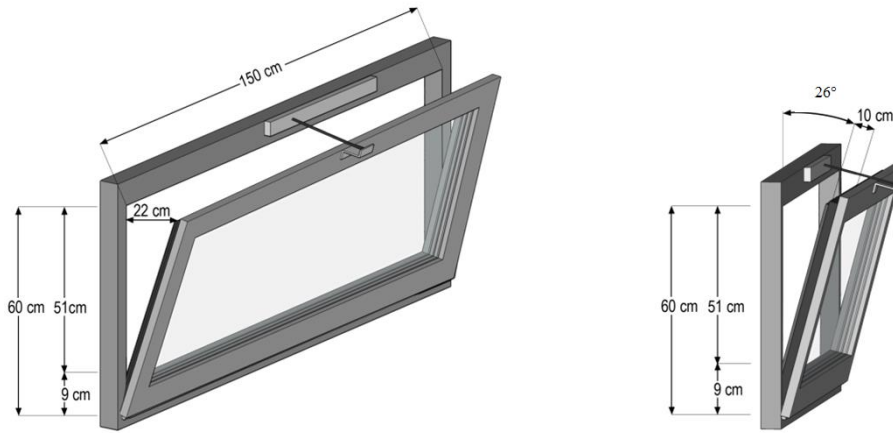


Figure 13: Isometric sketch of the tested window

Thereby, air change rate under different seasons are recorded for very different weather conditions. Measurements are performed for **single sided ventilation** only. For all measurements the heater is turned off. The correlation between pressure losses expressed by the discharge coefficient c_D , temperature differences ΔT and external wind speed u are formulated by Maas [12]:

$$\dot{V}_{in} = \dot{V}_{out} = 3600 * \frac{1}{2} A c_D \sqrt{C_1 u^2 + C_2 H \Delta T + C_3} \quad (3.1)$$

with $C_1 = 0.0056$ $C_2 = 0.0037 \text{ m}/(\text{s}^2\text{K})$ $C_3 = 0.012 \text{ m}^2/\text{s}^2$

It is assumed that the airflow occurs through one window and therefore the area for supply and exhaust air is 50% of the window area A . This equation allows calculating discharge coefficients for different climate conditions and measured air change rates.

To compare these measurements with the wind tunnel tests performed at *Unicamp*, it is intended to implement this window setup in EnergyPlus simulations for single sided ventilation (Chapter 4).

3.2 Comparison of different tracer gases

3.2.1 Desired properties of the tracer gas

Today there are several highly sensitive gas analyzers available on the market. Therefore, the choice of tracer gas is not only dependent on the laboratory hardware but also on the properties of the gas itself. Gases shall be chosen to avoid any interaction with existing ventilation systems or with passive airflow. Risk to human health or the environment arising from tracer gases must be prevented as good as possible. Hence, the following properties of tracer gases should be aimed [13]:

- Non-toxic for humans in the concentration range used,
- Without hazard to the environment,
- Non-existent in air or concentrations far below the concentration range used for measurements,
- Chemically inert. There should not be any reactions with air or other materials inside of the zone,
- Miscible with air,
- Walls, ceiling and furniture should not absorb the tracer gas,
- Detectable with available equipment.

Additionally, it is of advantage if the gas is inexpensive available on the market as well as easily transportable for mobile measurements. The following chapters give a short overview of commonly used tracer gases.

3.2.2 Carbon dioxide (CO₂)

Carbon dioxide is one of the components of air which is detectable and which can be quantified with little effort. The required equipment is reasonably priced. It must be taken into account that the background concentration of carbon dioxide in air varies between 350 – 400 ppm [14] depending on whether the measurement takes place in the city or countryside. The background concentration has to be recorded and subtracted from measured concentrations for accurate results. In occupied rooms, humans exhale CO₂ continuously. The CO₂ production rate for normal office activities is around 20 l/h per person [13]. This means, that 2 people will increase the CO₂ concentration of a 65 m³ room from 400 ppm (ambient outside air) to 1000 ppm (Pettenkofer value) within one hour which is the upper limit of hygienic air. For higher accuracy of results, the concentration used for measurements in occupied rooms should be noticeable above the background and human caused concentrations. Thus, it will cause restricted ability to concentrate, headache and in the worst case it can cause death by suffocating. Nevertheless, CO₂ fulfills a lot of above mentioned requirements for good tracer gases but it should be used with caution.

3.2.3 Sulfur hexafluoride (SF₆)

Sulfur hexafluoride is the most frequently used tracer gas in infiltration or ventilation measurements. It is almost the ideal tracer gas due to its properties. The concentration can be analyzed in extremely low concentrations (detection limit in air is 5 ppt) with high accuracy. The 'MAK-value', a tolerated value of gas concentrations at workplaces defined by the *Association of German Engineers* (VDI), is 1000 ppm as an 8-hours average value. Usually, the maximum concentration with tracer gas measurements does not exceed 100 ppb, which is a ten-thousandth of the permanently tolerated value. SF₆ can be used in occupied buildings without health problems for people. It is almost non-existent in ambient air (0.85-1.5 ppt) [13] so it does not influence the measurements. The density of SF₆ is 6.17 kg/m³ which is 6 times heavier than air. It is very important to thoroughly mix the gas with indoor air before starting the measurements in order to guarantee an equal distribution of tracer gas. The chemical properties also support the use of SF₆ as tracer gas. It is very stable and only decomposes above 550°C [15]. Due to this, it is very slowly degrading in the atmosphere. The greenhouse effect of SF₆ is more than 20,000 times higher than the effect of CO₂. Because of the extremely low background concentrations the global impact is low. However, it should be used wisely and in the lowest concentration suitable for the measurement.

3.2.4 Nitrous oxide (N₂O), Hexafluorobenzene (C₆F₆) and other tracer gases

There are a number of additional gases which are suitable for air change rate measurements in different dimensions. Since they are not considered in this research project, reference is made to further literature [13] [15] [16] [17].

3.3 Mathematical background

The tracer gas concentration in a defined space as a function over time can be formulated with the principle of mass conservation. It expresses that the mass of a system, i.e. the concentration of tracer gas in a room, can only change if it will be added or removed. Considering a concentration of tracer gas in the room air $C_i(t)$ it can be removed with the expression $\dot{V} * C_i$ and added with the amount of $\dot{V} * C_e$ by ventilation processes as well as with a constant emission of F with

C_i	Concentration of tracer gas in the room
C_e	Concentration of tracer gas of the exterior
\dot{V}	Airflow rate
F	Constant emission of tracer gas to the room.

Hence, the mass balance of tracer gas in a space with the volume V_S can be expressed as a differential equation [18]:

$$V_S \frac{dC_i(t)}{dt} = C_e \dot{V} + F - C_i \dot{V} \quad (3.2)$$

Dividing by V_S and replace \dot{V}/V_S by the air change rate n leads to the description of tracer gas concentration at the time t :

$$\frac{dC_i(t)}{dt} = C_e n + \frac{F}{V_S} - C_i n = (C_e - C_i) n + \frac{F}{V_S} \quad (3.3)$$

For the starting condition $C_i(0) = C_0$ and by integration it yields:

$$C_i(t) = C_e + \frac{F}{n V_S} + \left(C_0 - C_e - \frac{F}{n V_S} \right) e^{-n t} \quad (3.4)$$

This equation is the basis for analysis of tracer gas measurements where data are recorded as concentration over time curves.

3.4 Error Analysis

For analyzing the sampling distribution on N probes each sampling time Y and probe concentration X are related. The standard error of the regression line is calculated by:

$$\sigma_M = \sqrt{\frac{1}{N-2} \left[\sum (y - \bar{y})^2 - \frac{[(x - \bar{x})(y - \bar{y})]^2}{\sum (x - \bar{x})^2} \right]} \quad (3.5)$$

The result of linear regression is a calculated air change rate n with a predicted standard error σ_M

$$n \pm \sigma_M \quad [h^{-1}]$$

3.5 Tracer gas procedures

3.5.1 Concentration decay method

This is the most frequently used method for determining air change rates. It can be done with the minimum of technical effort. Before the measurement starts a defined mass of tracer gas is injected to the room (e.g. by gas tanks with pressure reducer or by using pre-filled syringes). The room air should be mixed manually in order to ensure an equal tracer gas concentration at each point inside in the room. As there is no additional emission of tracer gas into the room ($F = 0$), Equation (3.4) can be written as:

$$C_i(t) = C_e + (C_0 - C_e) e^{-n t} \quad (3.6)$$

In regular time intervals Δt probes of room air with the tracer gas concentration $C_i(t)$ are taken and analyzed in a gas chromatograph with an electron capture detector. For these investigations SF_6 tracer gas is used. SF_6 is almost non-existent in exterior air (0.85-1.5 ppt) [13] and therefore the expression can be simplified to:

$$C_i(t) = C_0 e^{-n t} \quad (3.7)$$

Due to ventilation, infiltration as well as air exchange with other rooms the concentration will decrease with time with exponential behavior. Determination of the air change rate n can be done by:

$$n = \frac{1}{t} \ln \left(\frac{C_0}{C_i(t)} \right) \quad \text{or} \quad n = \frac{1}{\Delta t} \ln \left(\frac{C_i(t)}{C_i(t + \Delta t)} \right) \quad (3.8)$$

Figure 14 illustrates the concentration over time curve of a concentration decay tracer gas measurement with the resulting $n = 2.54 \text{ h}^{-1} \pm 0.02 \text{ h}^{-1}$.

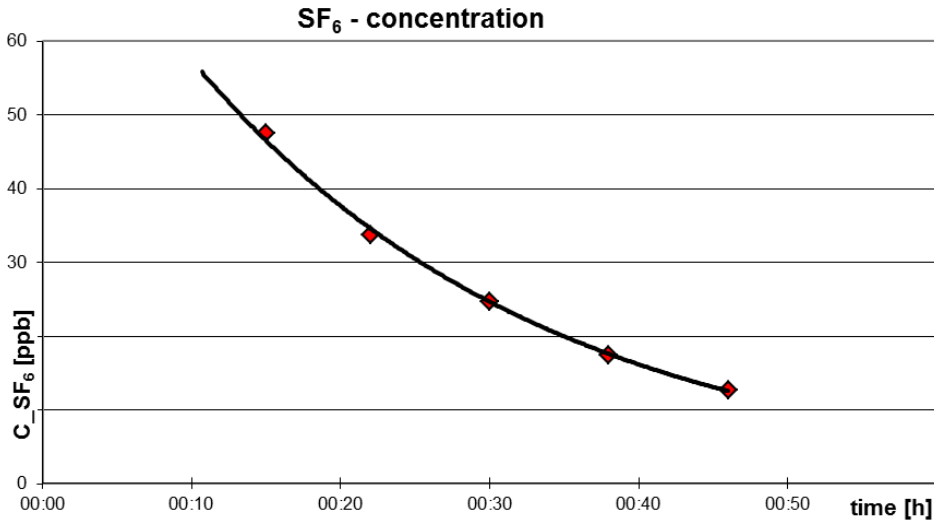


Figure 14: Typical graph of tracer gas concentration with concentration decay method

3.5.2 Constant emission method

In contrast to the concentration decay method here is a constant emission of tracer gas F . A defined amount of tracer gas is constantly emitted to the zone. The tracer gas concentration increases from the background concentration ($C_0 = C_e$) to an equilibrium concentration C_{eq} . This is reached when the tracer gas supply is equal to the tracer gas removal by ventilation processes. Thus, Equation (3.4) can be written as:

$$C_i(t) = C_e + \frac{F}{n V_S} + \left(1 - \frac{F}{n V_S}\right) e^{-n t} \quad (3.9)$$

Assuming that the time, until this concentration is reached, is much bigger than $1/n$, the part of the e-function becomes to zero and the concentration can be determined by the following equation where the background concentration C_e is almost zero and therefore negligible:

$$C_{eq} = C_e + \frac{F}{n V_S} \quad (3.10)$$

When the stable concentration of tracer gas is reached air samples can be taken and analyzed to determine the concentration and to calculate the air exchange rate by using Equation (3.10). If probes are taken before the equilibrium concentration is reached the air exchange rate will be overestimated [15]. An analysis for the time to reach the equilibrium concentration depending of the air exchange rate n is made in [15]. The behavior of the tracer gas concentration curve is shown in Figure 15.

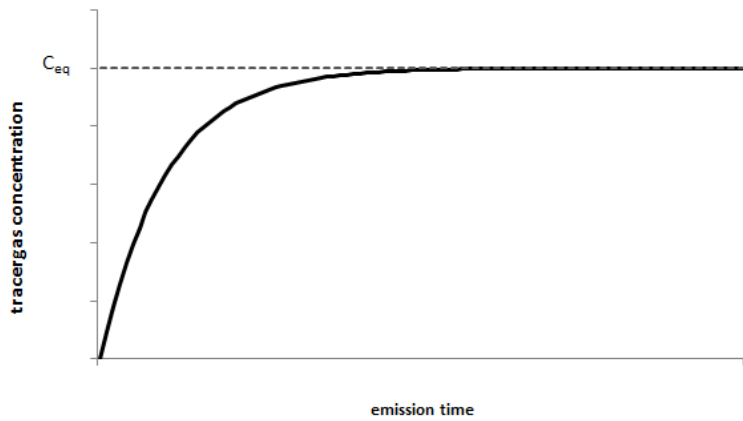


Figure 15: Typical graph of tracer gas concentration with constant emission method.

3.5.3 Constant concentration method

During the experiment a constant concentration of tracer gas in the zone is aimed. To maintain this, an automated dosing system connected to a gas analyzer is required. This method requires the most complex hardware but it enables long-term recording of air change rates and it also enables detection of temporarily fluctuations due to changing boundary conditions. The air change rate n can be calculated from the conversation of mass according to Equation (3.3). For an ideal tracer gas supply the concentration is exactly constant and therefore the derivation of tracer gas concentration as a function of time is zero:

$$\frac{dC_i(t)}{dt} = (C_e - C_i) n + \frac{F}{V_S} = 0 \quad (3.11)$$

Assuming tracer gas in external air is non-existent the airflow rate can be calculated by:

$$\dot{V} = \frac{C_i}{F} \quad (3.12)$$

3.6 Experimental setup and requirements for the measurement

In this study concentration decay method is used. The success of the tracer gas model described above depends on some prerequisites and assumptions which must be made:

- Injection of tracer gas should not change the density of the room air. The maximum concentration at the beginning of these experiments is lower than 50 ppb. This requirement is fulfilled.
- The tracer gas concentration C is supposed to be equal in the whole zone for a given time.
- To improve the mixing process, the SF₆ tracer gas is previously diluted in the laboratory to 20% concentration. Thereby, the density of the injected gas is reduced from 6.17 kg/m³ to 2.20 kg/m³ which enable a better mixing process.
- Homogeneous concentration presupposes that air and tracer gas are completely mixed throughout the experiment. The air exchange process does not influence the homogeneity of the air-gas-mixture. In fact there can be '*fresh air flushes*' nearby the windows.
- Objectively, the tracer gas concentration C is not totally equal. Due to supply airflow the concentration near the windows is expected to be lower than in the interior room corners. In order to meet the requirements the probe is taken from different points in the room. While the probe is drawn into the syringe the position and height inside of the room is changed (see Figure 16).
- Changes in tracer gas concentration should only occur due to the air exchange with the exterior. Two doors to adjacent rooms are sealed during the measurements. The infiltration was determined to 0.30 h⁻¹.
- Finally the standard error of the probes is determined to verify the assumptions (i.e. homogeneous mixing of tracer gas and air).

This method provides an average air change rate during the measurement duration for single-sided ventilation. The duration is dependent on the space air volume and the estimated airflow rate. For this study the duration is around 45 minutes.

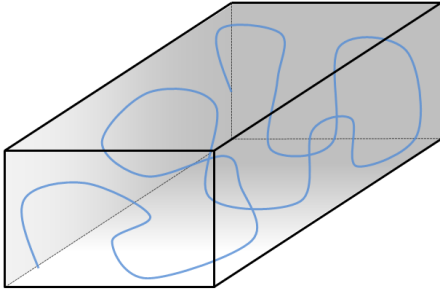


Figure 16: Exemplary path of probe-taking by using a syringe

Measurements of air change rate have been conducted in an office room of the *HCU* under varying environmental conditions.

3.7 Weather conditions

In total, 20 measurements of air change rate with different climate conditions are done. The weather conditions are recorded as an average value during the experiment. Figure 17 plots an overview of the temperature difference between the office room and outdoor (positive value means indoor temperature above outdoor temperature) and the wind speed measured in front of the facade. All values are mean values for the measurement duration of around 45 minutes. The wind direction is discussed below.

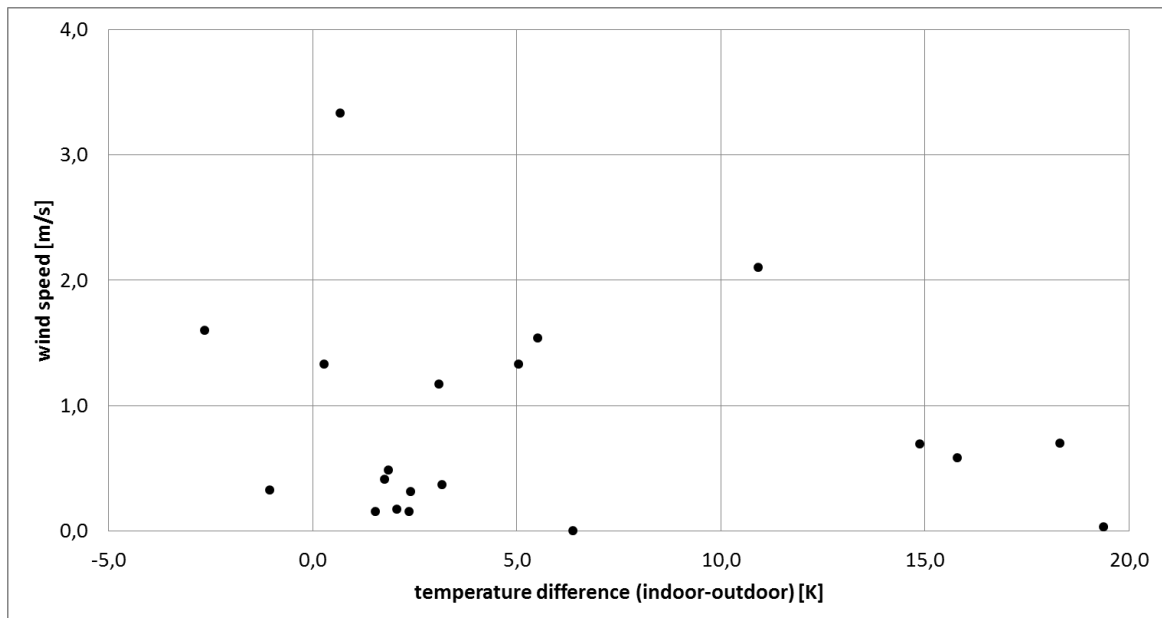


Figure 17: Weather conditions during the tracer gas measurements

Wind distribution in Hamburg is strongly influenced by South-West wind. Figure 18 shows the wind rose for the city of Hamburg based on the *IWEC* (International Weather for Energy Calculations) hourly averaged data.

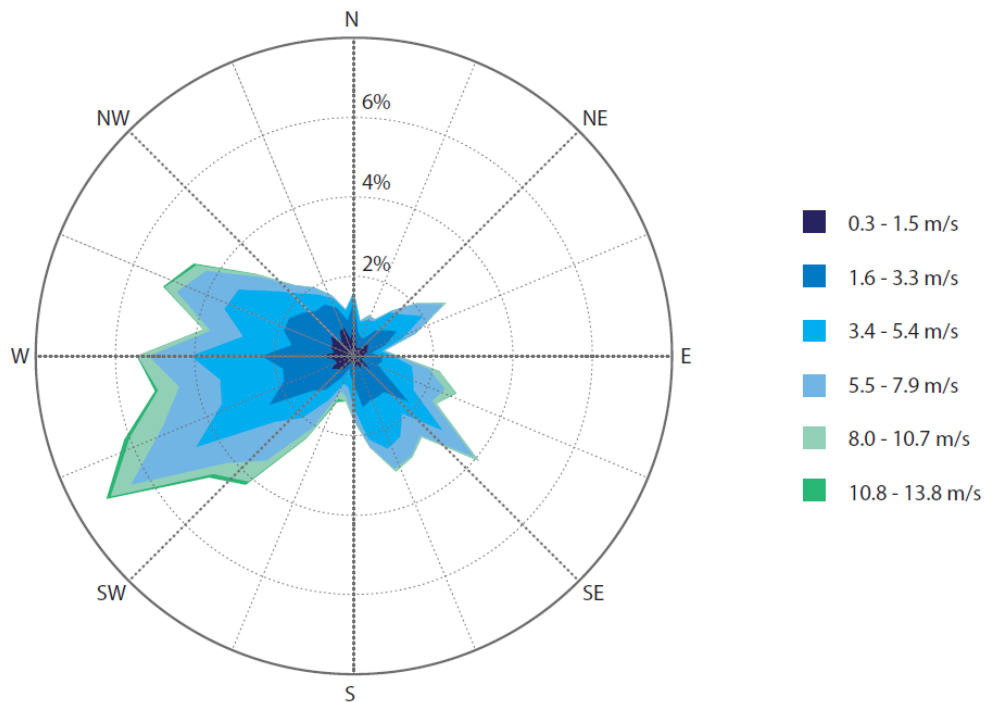


Figure 18: Wind speed and direction in Hamburg

Due to the east-west orientated building shape and the dominating wind direction recorded data for wind direction in front of the facade are clustered in four groups:

- Wind from South-West to West (225-270°) 41% occurrence frequency
This is named as parallel wind conditions
- Wind from East to North-East (45-90°) 23% occurrence frequency
- Wind from South to South-West (180-225°) 11% occurrence frequency
This is named as wind conditions perpendicular to the facade
- Wind from North to North-East (0-45°) 10% occurrence frequency
This wind direction does only occur due to strong turbulences. The building envelope prevents the sensor of recording wind from the North.

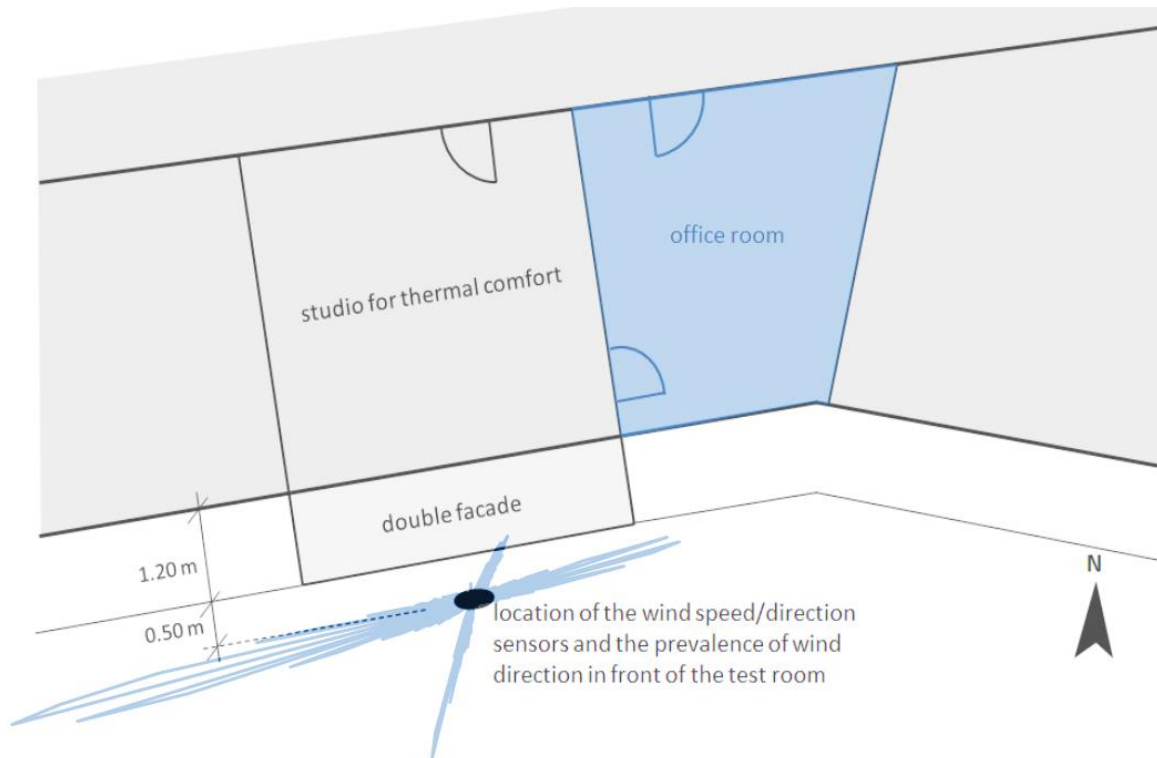


Figure 19: Floor plan of the test office and wind rose in front of the facade

3.8 Results

The following table gives an overview of the average weather conditions during the measurements and the corresponding air change rate ACH . The ID refers to the number in the diagrams (Figure 20 and Figure 21).

Table 6: Results and weather data for the tracer gas measurements

ID	ΔT [K]	v [m/s]	wind direction [°]	ACH [h ⁻¹]	ID	ΔT [K]	v [m/s]	wind direction [°]	ACH [h ⁻¹]
1	1.55	0.15	140	1.16	11	0.29	1.33	147	4.56
2	-1.04	0.32	148	1.72	12	1.77	0.41	178	2.02
3	5.51	1.54	254	4.17	13	2.40	0.31	141	1.78
4	5.06	1.33	256	2.54	14	6.38	0.00	244	1.53
5	0.68	3.33	258	5.28	15	-2.65	1.60	254	3.08
6	1.87	0.48	209	2.22	16	19.38	0.03	153	2.07
7	2.37	0.15	178	1.71	17	18.31	0.70	262	2.43
8	3.10	1.17	116	3.43	18	14.89	0.69	257	2.15
9	3.17	0.37	73	3.19	19	15.80	0.58	207	2.28
10	2.07	0.17	226	1.36	20	10.93	2.10	255	3.51

A linear dependency between wind speed v and resulting air change rate ACH is found (see Figure 20). This dependency is confirmed by the orifice equation where the linearity can be seen. For both parallel and perpendicular wind flow an equation is formulated by linear curve fitting. The constant term, representing the airflow without wind, is around 1.40 ACH for both cases which is a good match of the measurements. The gradient of the curve for perpendicular wind flow is almost twice the gradient of the curve for parallel wind flow which emphasized the wind pressure distribution on facades known from previous studies [19].

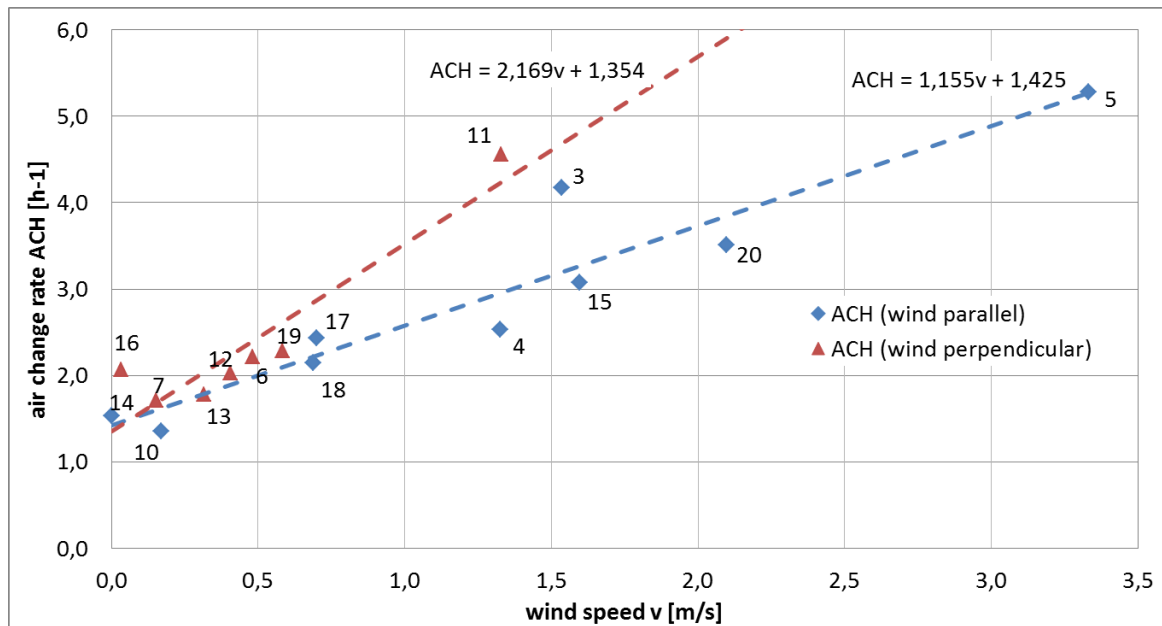


Figure 20: Air change rate depending on the wind speed for parallel and normal wind conditions

Figure 21 shows the air change range depending on the temperature difference between the office room and outdoor. No clear behavior can be found. This proves that pressure differences from wind flow are the dominating forces in most passive ventilation processes.

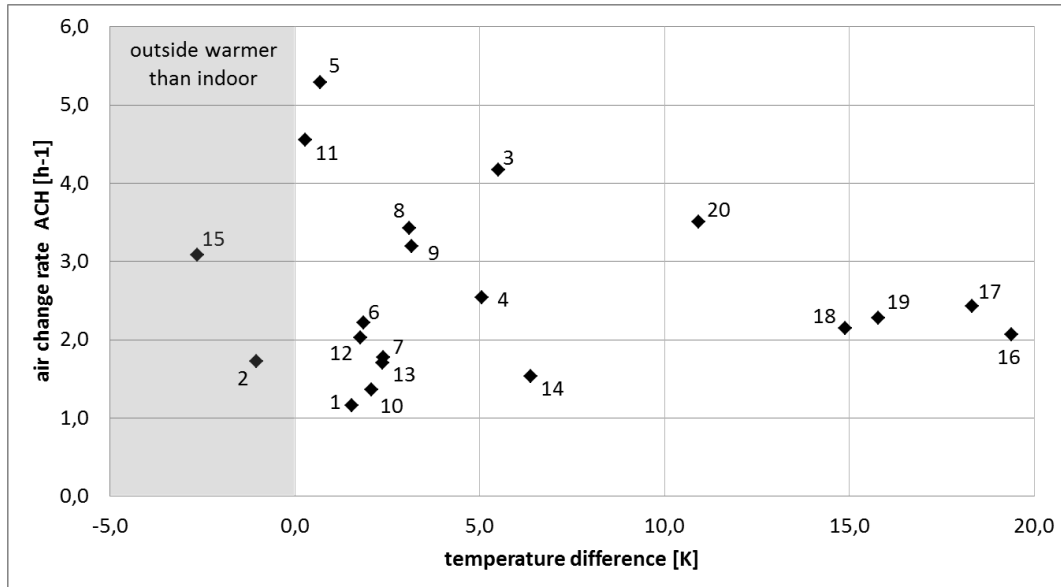


Figure 21: Air change rate depending of temperature differences

Figure 20 shows a strong dependency between airflow through the window and wind flow direction. The approach developed by Maas (see Equation (3.1)) does not cover different incidence angles. Accurate discharge coefficients cannot be calculated with this formula.

Moreover, the results show a high degree of scattering. Changing boundary conditions during the experiment like wind turbulences, shading due to clouds or increasing solar radiation may be one reason for this. The calculation of coherent discharge coefficient(s) for this window type is not possible with results obtained from measurements.

3.9 Conclusion

A linear dependency between wind speed v and resulting air change rate ACH is found (see Figure 20). However, it is not possible to calculate a generic discharge coefficient with this data. To gain appropriate discharge coefficients as input for thermal building simulations several recommendations can be given with the experience from these measurements.

The concentration decay method is the simplest way to measure the air exchange rate in buildings. The total amount of 20 measurements is not enough to cover all seasons at the wide range of weather conditions which occur. More measurements should be done. However, concentration decay method provides an average air change rate during the time of the measurement. In the present study the total duration was around 45 minutes. Weather conditions change within this time especially wind fluctuations can change within seconds. For academic use this method might not be suitable to cover the high demands of accuracy. As shown in [20] and [21] constant emission method allows measurement of air change rate multiple times per second and it reveals about the relation between suddenly changing weather conditions and air exchange rate.

4 Computer modeling and results analysis

4.1 Methods

The energy performance and user thermal comfort in naturally ventilated spaces can be estimated for different climate zones by using a building energy simulation program. The computer models for this research are developed and run in EnergyPlus. With known discharge coefficients, calculated from wind tunnel experiments (see Chapter 3), natural ventilation can be implemented. The purpose of the simulations is to evaluate the thermal and energetic performance of a room with the different types of windows tested in the wind tunnel. With these results the design guidelines for retrofitting of buildings are developed.

All rooms are simulated with natural ventilation if possible and with an HVAC cooling system if necessary (see Chapter 4.3 for details). Due to the air conditioning system discomfort is limited to a very low number of hours and therefore negligible. Well-designed natural ventilation reduces the runtime and energy consumption of artificial cooling. The characterization of the efficiency of natural ventilation is done by comparing the energy demand for cooling for all situations.

4.2 Building description

The thermal zone under investigation is a room based on the study carried out in a building of the Ministry of the Environment and Ministry of Culture, located in Brasilia, Brazil [22] with dimensions based on BESTTEST 600 (6.00 x 8.00 x 2.70 m). BESTTEST is a method for testing and diagnosing of building energy simulation programs developed in the Annex 43 *Testing and Validating Buildings Energy Simulation Tools of Energy Conservation in Community and Community Systems and Buildings Programme* (EBC) of the *International Energy Agency* (IEA) [23].

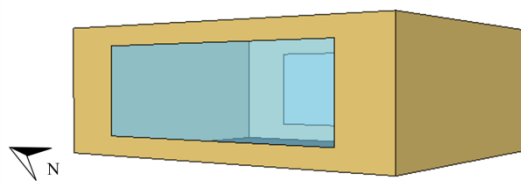


Figure 22: Schematic view of the zone

The zone is located on an intermediate floor. East and west facades are in contact with the external environment (Figure 22). The opaque area of the external facade is modeled with a thickness of 15 cm and with a transmittance of $1.40 \text{ W}/(\text{m}^2\text{K})$ (concrete block wall with air gap). The transmittance value adopted for the envelope of the zone is similar to the value used in simulations carried out for the study about the energy efficiency labelling of the existing building of the Ministry of the Environment and Ministry of Culture, located in Brasília, Brazil [22].

External blinds are used to compare the thermal behavior of the room with and without shading. In the case that shading is used a solar radiation setpoint of 180 W/m^2 on the window surfaces enables the shading. The blinds are modeled with horizontal slat orientation, dark color, slat width of 0.09 m , slat to slat separation of 0.08 m , and slat thickness of 0.001 m , slat angle of 5° , conductivity of 150 W/(mK) , visible transmittance of 0 and maximum slat angle of 180° .

The zone operates according to specific schedules of metabolic rates, lighting and equipment power, based on [22]. The description of the scenario used in the present study is summarized in Table 7. The lighting and equipment schedules are set according to the occupancy schedule.

Table 7: Operation schedules of the Ministry of Culture

Occupation	5 people (in a room with 48 m^2 floor space)
Occupancy schedule	For weekdays: From 8:00 a.m. to 12:00 a.m. and from 2:00 p.m. to 6:00 p.m.
Metabolic rate	130 W/person
Lightning power	7.97 W/m^2
Equipment power	24.33 W/m^2

4.3 EnergyPlus and MATLAB Co-Simulation

An external interface is used to couple EnergyPlus and MATLAB. This method provides control possibilities which are not feasible in EnergyPlus alone. Based on simulation results for timestep (i) MATLAB will calculate schedule values and setting parameters for artificial cooling and natural ventilation. These parameters will be written back to EnergyPlus for timestep (i+1). This way an adaptive schedule and control algorithms are created for permanently changing boundary conditions.

Figure 23 shows the program sequence. In the first step the program checks if the room is occupied. In order to avoid uncomfortable room conditions during the first timesteps each morning the definition of *Occupancy* also includes 15 minutes before people start working as well as the lunch break. If the room is not occupied, the HVAC systems are turned off in order to save energy. If it is not *too cold* and the zone air is warmer than the external air, the windows will open (this case occurs for night cooling). If the room is occupied, the program checks whether the operative temperature is *too warm*, *warm*, *cold* or *too cold* according to the ASHRAE 55 adaptive comfort model (see Figure 24). The definition of *too warm* starts 0.1 K before the line of 80% acceptance in order to start the air conditioning in time. Thus, the turn-ons of the system and the hours of discomfort can be further reduced.

Based on the classification in this comfort model and by comparing the internal and external air temperature decisions are made for both natural and artificial ventilation. The algorithm sends an *availability schedule* value (true/false) to EnergyPlus. EnergyPlus enables the system if the schedule allows.

Because of the method of co-simulation with EnergyPlus and MATLAB, there is a compulsorily delay of one timestep for the settings, i.e. the best settings for timestep (i) will be used to control natural ventilation and air conditioning in timestep (i+1). Since the timestep is chosen to 5 minutes (see Chapter 4.5), the delay is short and tolerable.

4.4 Parameter study

In order to analyze the impact of discharge coefficients on natural ventilated buildings in different boundary conditions a comprehensive set of parameters is chosen for thermal building simulations. Table 8 provides an overview about the parameters. All of these parameters are combined with each other to a total of 2,048 evaluated simulations. The simulation settings affiliated to these parameters are described below.

Table 8: Overview of parameter variation

Bioclimatic Zone	Window Wall Ratio	Window Types	c_D (close)	c_D (open)	Shading	Cooling Setpoint	Glazing
1 – Curitiba	25 %	Maxim-ar 45°	0.001	0.578	none	constant	single
2 – Uruguaiana	50 %	Maxim-ar 90°	0.001	0.721	blinds	ASHRAE	double
3 – São Paulo	75 %	Boca de Lobo Fixo	0.183	0.183			
4 – Brasília	100 %	Veneziana Flaps	0.079	0.226			
5 – Niterói		Veneziana Holes	0.021	0.212			
6 – Goiânia		Parallelausstellfenster	0.001	0.180			
7 – Cuiabá		Dreh-Kipp-Fenster	0.001	0.107			
8 – Belém		Dachfenster	0.001	0.113			

Bioclimatic Zones

Brazil is divided in eight bioclimatic zones. The definition of zones and classification of 330 cities is made in the Brazilian standard NBR 15220-3 [24]. The standard also provides recommendations for ventilation openings, shading and strategies for passive thermal conditioning. Required characteristics for the openings in the studied zones are summarized in Table 9. Figure 25 gives a visualization of the country and its bioclimatic zones. The weather files used for thermal simula-

tions are compiled by *INMET - Instituto Nacional de Meteorologia*. An analysis of air temperatures (monthly average as well as average high/low) and precipitation is given in Figure 26.

Table 9: Design guidelines for the studied zones based on NBR 15220-3

Zone	City	Recommendations
Z1	Curitiba	Openings with medium dimensions and avoiding shading during the winter for solar gains. Use of external walls and roofs of low thermal inertia and insulated roof. During the winter time, the use of solar heating and internal walls with high thermal inertia.
Z2	Uruguaiana	Openings with medium dimensions, shading but allowing the winter sun to enter the room and need for cross ventilation during the summer. Use of external walls and roofs with low thermal inertia and insulated roof. During the winter time, use of solar heating and internal walls with high thermal inertia.
Z3	São Paulo	Openings with medium dimensions, shading but allowing the winter sun to enter the room and need for cross ventilation during the summer. Use of external walls and roofs of low thermal inertia, reflective walls and insulated roof. During the winter time, use of solar heating and internal walls with high thermal inertia.
Z4	Brasília	Openings with medium dimensions, shading during the whole year. Use of heavy walls and lightweight roofs with thermal insulation. Use of evaporative cooling, thermal inertia for cooling and selective ventilation during the summer. Solar heating and high thermal inertia of the internal walls during the winter.
Z5	Niterói	Openings with medium dimensions, shading and need for cross ventilation during the summer. Use of light and reflective walls, light insulation and roofs with thermal insulation and internal walls with high thermal inertia during the winter.
Z6	Goiânia	Openings with medium dimensions and shading. Use of heavy walls, roofs with thermal insulation, use of evaporative cooling and selective ventilation during the summer, and use of heavy internal walls during the winter.
Z7	Cuiabá	Openings with small dimensions and shading during the whole year. Use of heavy walls, roofs with thermal insulation, use of evaporative cooling and selective ventilation during the summer, and use of heavy internal walls during winter.
Z8	Belém	Openings with big dimensions, shading and allowing cross ventilation during the whole year. Use of heavy walls and roofs.

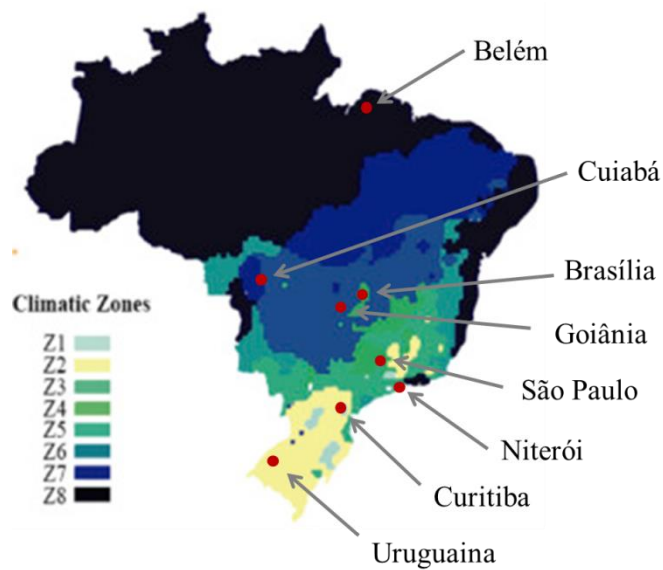


Figure 25: Bioclimatic zoning of Brazil (adapted from [25])

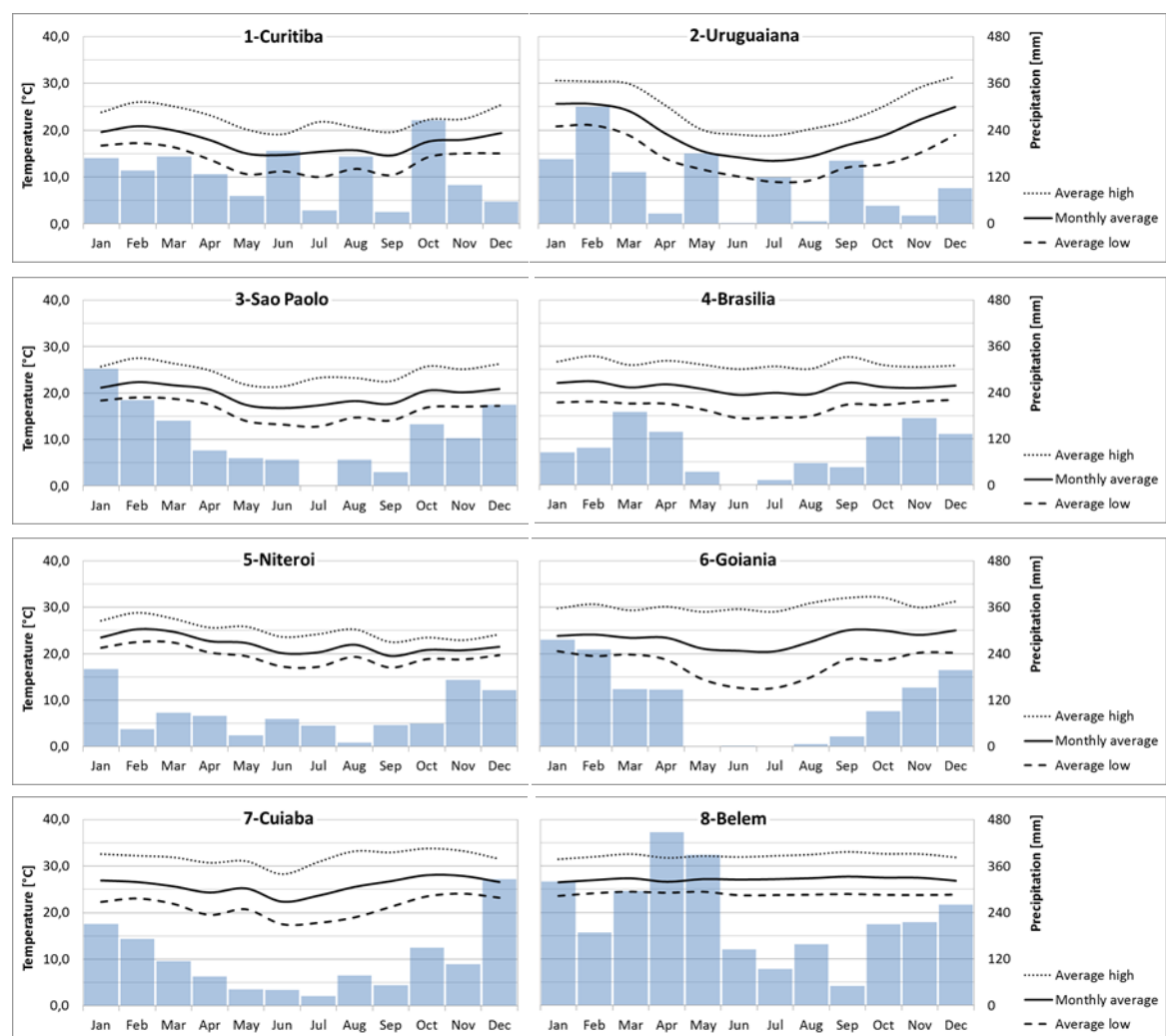


Figure 26: Temperature and precipitation in eight Brazilian cities

Window Wall Ratio

While big windows allow higher air mass flow through open windows they also gain solar radiation if not shaded. To analyze the impact of window wall ratio, four different values are chosen for both east and west facade to represent various field of building applications. It should be noticed that even the highest percentage of glazing includes a thin opaque window frame.

Window Type

The previously studied windows are analyzed in numerical models. For common Brazilian and German windows a discharge coefficient of 0.001 is chosen for closed windows. For open conditions the discharge coefficient determined in wind tunnel is used. For *Veneziana* windows both discharge coefficients for open and closed windows are measured. *Boca de Lobo Fixo* window is designed for hot and humid climate. This window is permanently open.

The wind tunnel setup allows determination of pressure losses for cross ventilation only, because the air streams through the openings in one direction. Therefore, all simulations are made for cross ventilation.

Shading Type

Two cases are studied: without any shading as well as with an external blind system. If shading is used, the shading automatically closes to cut-off position when the radiation on the window surface exceeds 180 W/m².

Cooling Setpoint

The EnergyPlus cooling setpoint represents an air temperature which should be ensured when the HVAC system is turned on. The comfort evaluation based on ASHRAE 55 is performed based on the operative temperature which is defined as the mean value of room air temperature $T_{air,in}$ and the mean temperature of the surrounding surfaces $T_{radiant}$.

$$T_{operative} = 0.5 (T_{air,in} + T_{radiant}) \quad (4.1)$$

To ensure an operative temperature for thermal comfort, a target air temperature is calculated based on the room performance for each timestep. An offset of 3.5 K is used to rise the temperature from the ideal value to the line of 80% acceptance. Thus, the energy demand for cooling is reduced significantly. However, it is the choice of the designer to define an increase of operative temperature taking into account the requirements inside of the building. This target air temperature is used for the HVAC control in EnergyPlus. The offset of one timestep between reading of values from EnergyPlus and writing of setpoints to EnergyPlus represents a hysteresis for the HVAC control system.

$$T_{air,target} = (T_{operative} + 3.5) * 2 - T_{radiant} \quad (4.2)$$

Two setpoints for air conditioning are studied:

- a) Fixed for air temperature = 24°C

If the algorithm allows cooling (see Figure 23), a constant cooling setpoint of 24°C is set.

- b) Based on ASHRAE 55 comfort model

Based on the room conditions for timestep (i) the cooling setpoint is calculated in order to meet the ideal ASHRAE 55 operative temperature (center of the comfort zone) based on Equation (4.2). For timestep (i+1) this setpoint is written to EnergyPlus.

4.5 Influence of timestep

The timestep is used in the EnergyPlus heat balance calculation. It represents the duration between two simulation steps or viewed reverse the number of intermediate calculations within one hour. The valid range is between 1 and 60 minutes. The choice of this is a choice about the accuracy of results. As the MATLAB algorithm produces a delay of one timestep between readings and writing of results, a short timestep, i.e. many steps of calculation, will reduce the real delay. However, simulation runtime increases with short timestep.

An evaluation of accuracy is previously made for a small set of chosen parameters. Two exemplary windows are analyzed in all climates for a window wall ratio of 50%. The influence of shading and HVAC setpoint is also under consideration.

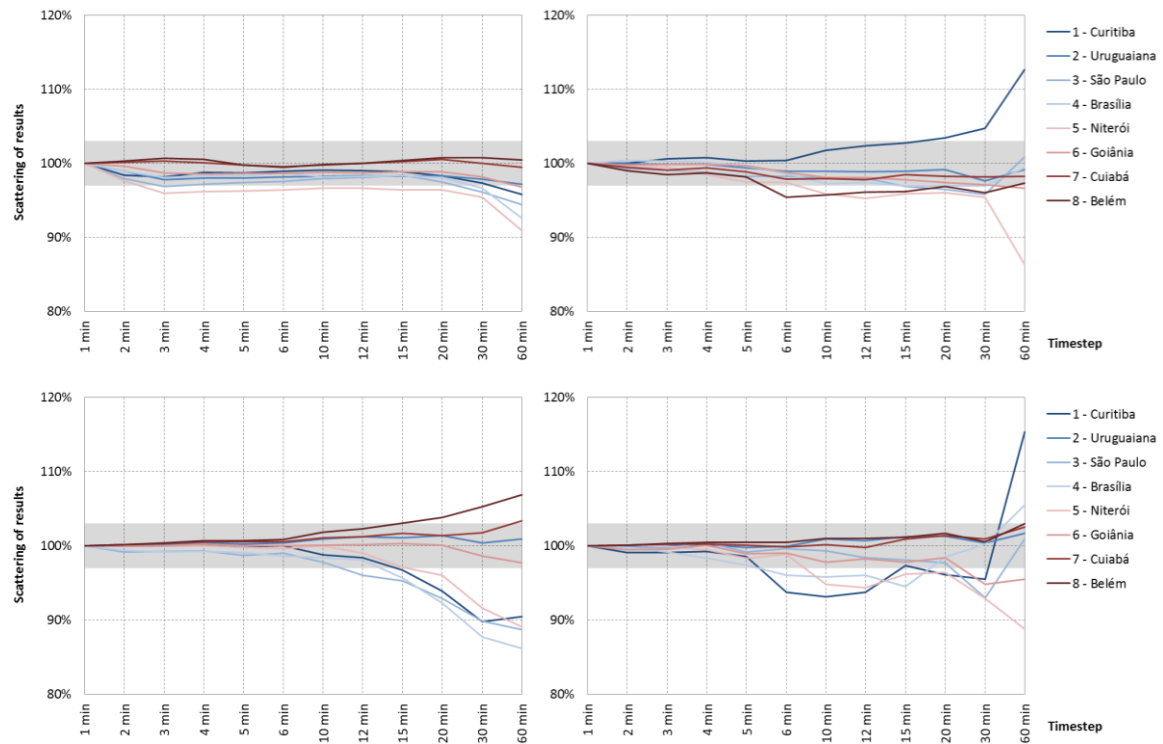


Figure 27: Influence of the timestep to simulation accuracy with Dreh-Kipp-Fenster
Left diagrams: without shading **right diagrams: with external blinds**
Upper diagrams: HVAC setpoint constant 24°C **lower diagrams: ASHRAE 55 setpoint**

Figure 27 shows the annual cooling load in percentage of the simulation with the highest resolution of timesteps for the Dreh-Kipp-Fenster window. The highlighted area shows an acceptable deviation of $\pm 3\%$. It can be seen, that the results of timesteps in a range from 1 to 5 minutes are close together. For higher timesteps the results are very different.

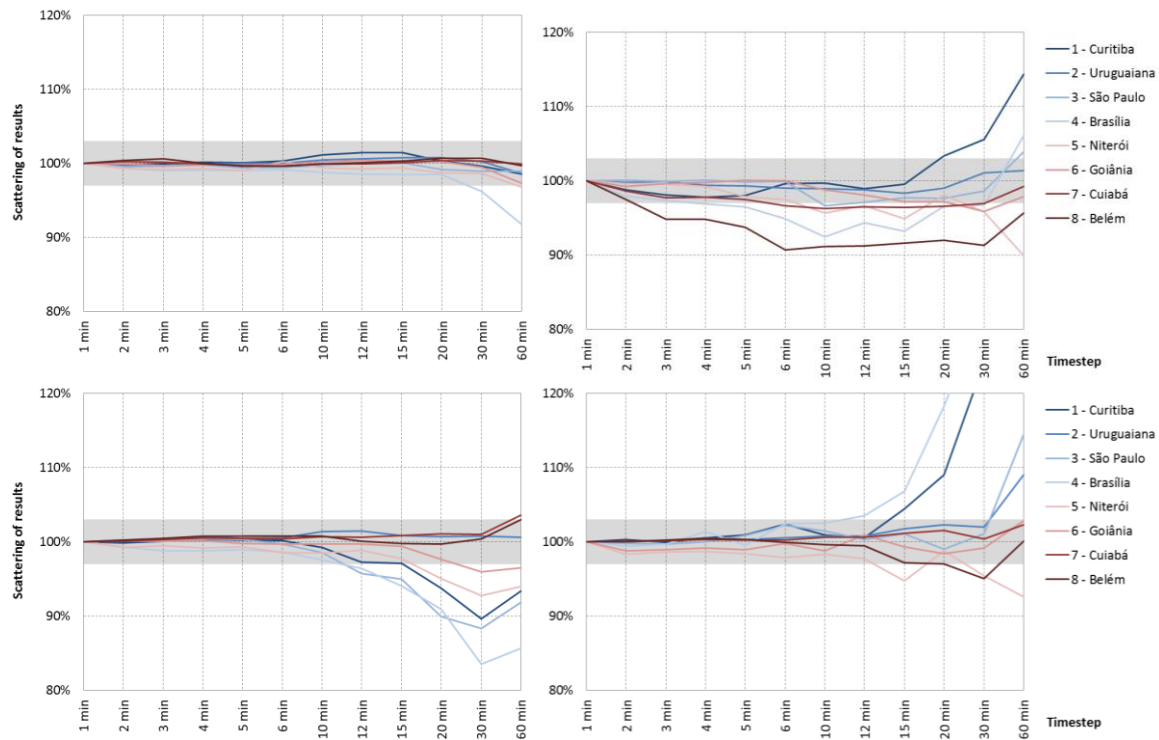




Figure 28: Influence of the timestep to simulation accuracy with Maxim-ar 45°
Left diagrams: without shading **right diagrams: with external blinds**
Upper diagrams: HVAC setpoint constant 24°C **lower diagrams: ASHRAE 55 setpoint**

Figure 28 shows the distribution of accuracy for the Maxim-ar 45° window. These results confirm the choice of timestep. For timesteps in a range from 1 to 5 minutes are close together. For higher timesteps the results are very different. In order to reduce the computation time needed, a timestep of 5 minutes, i.e. 12 intermediate calculations per hour, is chosen for further investigations.

4.6 Glazing type

Single glazed windows are state of the art for many Brazilian buildings. They are reasonably priced and they do not have high requirements for the window frame. An insulated building envelope is often not necessary in warm climates. However, if an air conditioning system is used, the interior air temperature might be below the outside air temperature. If the outside temperature exceeds the interior for long periods within a year, the use of insulated and coated glazing should be considered. The properties of the two glazing types are shown in Table 10.

Table 10: Properties of glazing types

Type	Section	U-Value	g-value
Single glazing	 Out In 4 mm clear glazing	5.80 [W/(m ² K)]	0.86 [-]
Double glazing	 Out In 4 mm clear glazing 14 mm gap (90% argon, 10% air) 4 mm coated glazing	1.22 [W/(m ² K)]	0.60 [-]

4.7 Results

In total 2,048 parameter variations are analyzed. It is not purposeful to show graphs for each case. In order to make clear and reliable statements the following chapters respond to the influence of chosen parameters. Building on that, recommendations for each climate are given. Detailed results with quantitative values for energy demand for cooling are shown in the appendix.

4.7.1 Influence of permanent ventilation

Three window types are characterized by permanent ventilation:

- Boca de Lobo Fixo contains two fixed parallel panes with a gap in between. This window cannot be adjusted to changing climate conditions. The discharge coefficient used in EnergyPlus simulations for all situations is constantly 0.183.
- Veneziana (Flaps and Holes) windows are sliding windows which can be opened and closed. In closed condition remain small openings in the form of flaps/holes for ventilation. Therefore, two different non-zero values for the discharge coefficient are used: Veneziana Flaps 0.079/0.226 and Veneziana Holes 0.021/0.212.

Permanent ventilation in combination with air conditioning increases the energy demand for cooling significantly because the conditioned air can leave the room at any time and warm air will enter the room. Figure 29 exemplarily shows the annual cooling load for an unshaded room in Curitiba with a constant cooling setpoint of 24°C. It can be seen that the results are in different

orders of magnitude. A direct comparison between the window types is not recommended because the natural ventilation situations differ a lot.

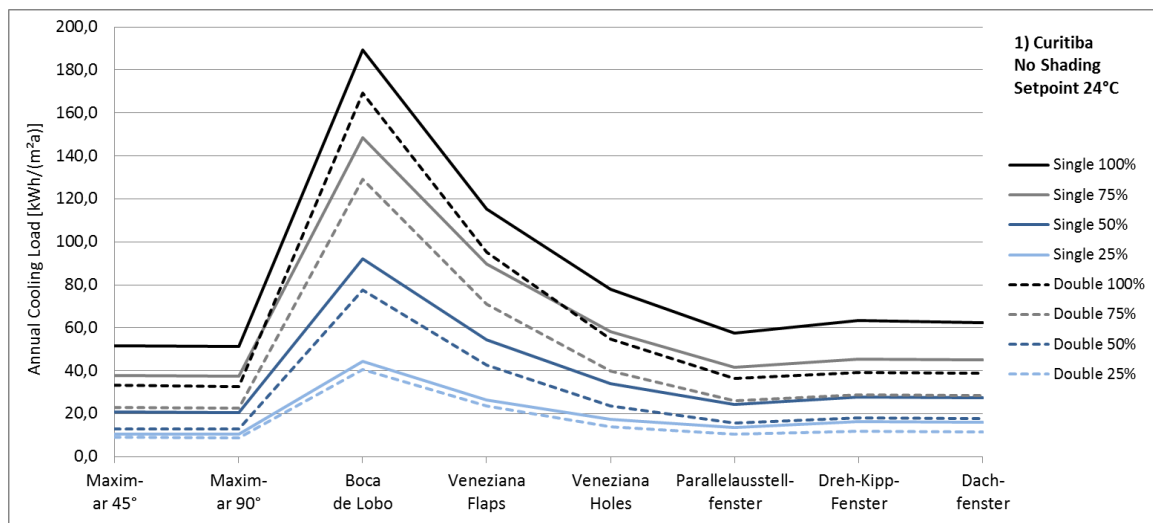


Figure 29: Annual cooling load (climate 1, no shading, constant setpoint)

Nevertheless, permanent ventilation can be a reasonable measure in hot and humid climates where buildings are not equipped with air conditioning (e.g. dwellings).

4.7.2 Influence of shading

The effect of external blinds is analyzed. The shading system closes when solar radiation on the vertical window surface exceeds 180 W/m². Table 11 summarizes the average energy saving for air conditioning (for all window types and for window wall ratios between 25% and 100%) if an external shading system is used compared to the same models without shading.

Table 11: Average energy saving for air conditioning when shading is used

Climate	Single Glazing		Double Glazing	
	Setpoint 24°C	ASHRAE	Setpoint 24°C	ASHRAE
1) Curitiba	53%	81%	41%	79%
2) Uruguaiana	39%	58%	34%	52%
3) São Paulo	46%	70%	37%	65%
4) Brasília	56%	83%	42%	81%
5) Niterói	48%	64%	41%	59%
6) Goiânia	39%	62%	34%	59%
7) Cuiabá	29%	45%	27%	41%
8) Belém	28%	43%	28%	40%

It can be seen, that the percentage of energy saving is higher in the southern climates 1 to 6. Climate 7 and 8 are characterized by high temperatures throughout the year as well as high humidity. In addition, the northern climates are close to the equator which leads to a high solar altitude during midday. Thus, the solar radiation on vertical window surfaces is comparatively low. Nevertheless, it should be mentioned that the values shown in Table 11 are percentages. The absolute energy saving [kWh/(m²a)] can be higher in northern climates due to the very high cooling load in general.

4.7.3 Influence of glazing type

Clear single glazing and a double glazing unit are compared. Positive effects of insulated glazing are a noticeably lower g-value whereby the solar transmittance can be significantly reduced as well as a lower U-value which decreases the heat gains. In hot climates, it often occurs that the outdoor air temperature exceeds the room air temperature, especially when the building is operated with air conditioning systems. In these situations, an insulated glazing will reduce the heat transmittance from outdoor to indoor. On the other hand, in moderate climates a lower U-value will reduce the heat loss during the night which might decrease the indoor temperatures during the day. In moderate climates it has to be weighed very carefully if a heater becomes necessary if the building envelope is not insulated.

Table 12: Average energy saving for air conditioning when double glazing is used

Climate	With Shading		No Shading	
	Setpoint 24°C	ASHRAE	Setpoint 24°C	ASHRAE
1) Curitiba	9%	39%	28%	45%
2) Uruguaiana	13%	23%	20%	31%
3) São Paulo	13%	31%	27%	40%
4) Brasília	4%	42%	31%	49%
5) Niterói	18%	29%	28%	38%
6) Goiânia	15%	29%	21%	34%
7) Cuiabá	14%	20%	16%	26%
8) Belém	16%	19%	15%	23%

In all climates, insulated glazing has a high potential to reduce the cooling load. The one-time investment in double glazing will pay off due to the annual energy saving. It should again be emphasized that Table 12 compares rooms with clear single glazing and a double glazing unit. It does not mean, that the adaptive setpoint based on ASHRAE leads to higher energy saving. It says

that if the cooling setpoint is chosen to be adaptive, the effect of double glazing is significantly higher.

4.7.4 Influence of air conditioning setpoints

It is being investigated how a constant setpoint for air conditioning of 24°C and an adaptive setpoint based on the ASHRAE adaptive comfort model do perform. Equation (4.2) explains how the adaptive cooling setpoint is defined. Table 13 states that high energy savings for cooling are possible. It also shows some values (highlighted with *) where a detailed consideration of each result show negative values which means a higher energy demand for cooling. The reasons for increasing and decreasing energy demand are describes below.

Table 13: Average energy saving for air conditioning when an adaptive cooling setpoint is used

Climate	Single Glazing		Double Glazing	
	With Shading	No Shading	With Shading	No Shading
1) Curitiba	51%	-4% *	67%	18% *
2) Uruguaiana	30%	1% *	38%	14% *
3) São Paulo	42%	1% *	54%	17% *
4) Brasília	57%	9% *	74%	29% *
5) Niterói	31%	0% *	40%	14% *
6) Goiânia	47%	16% *	56%	29%
7) Cuiabá	34%	15%	38%	24%
8) Belém	34%	17%	35%	25%

For most of the cases (in 888 of 1,024 comparisons) the ASHRAE based setpoint leads to a noticeably reduction of energy demand for air conditioning. ASHRAE defines the comfortable temperature range in dependence of the outdoor temperature which is often above 24°C by which the temperature difference between the room air temperature and the target temperature is lower most of the time. On the other hand, a constant setpoint of 24°C for the indoor air temperature can lead to uncomfortable and uneconomical cold temperatures.

Increased energy demand for cooling occurs only if no shading is used. A detailed analysis of the simulation results shows, that a low solar altitude leads to high surfaces temperatures if no shading is used. Comfort analysis is based on the operative temperature which is defined as the average value of mean surface temperatures and air temperature. If the surfaces are very warm, the air temperature needs to be lower in order to keep the operative temperature inside of the comfortable range. As a result, an air temperature of 24°C, which is aimed in case of the constant setpoint, does not obtain thermal comfort. On the opposite, the adaptive setpoint enables lower air tempera-

tures in order to obtain thermal comfort but this results in higher energy demand. It can be shown, that the choice of *no shading* is the reason for increasing energy demand for cooling.

4.7.5 Design recommendations

Typical office rooms in Brazil with air conditioning are analyzed. All rooms are ventilated purely naturally. In order to guarantee thermal comfort at any time when the room is occupied an artificial cooling system is used for all simulations. The efficiency of natural ventilation can be expressed by the energy demand for cooling.

It turned out that, independent of the bioclimatic zone, the following parameters will reduce the energy demand for cooling:

- Smaller windows significantly reduce the energy demand for cooling,
- The use of an external shading system is recommended for all climates,
- A double glazing unit reduces solar gains noticeable and therefore the energy demand for cooling decreases as well,
- An adaptive cooling setpoint (discussed in Chapter 4.4) is preferable to a constant cooling setpoint.

When the above mentioned design recommendations are followed, the choice of the window type plays a subordinate role. The window type Maxim-ar 90° leads to the lowest energy demand for cooling in all climates, because the discharge coefficient and thereby the air change rate as well are the highest of all tested windows. However, permanent ventilating window types should not be used when an air conditioning system is used.

The following figures show the annual energy demand for cooling for each climate considering the above mentioned parameters. Detailed results with quantitative values for energy demand for cooling for all cases are shown in the appendix.

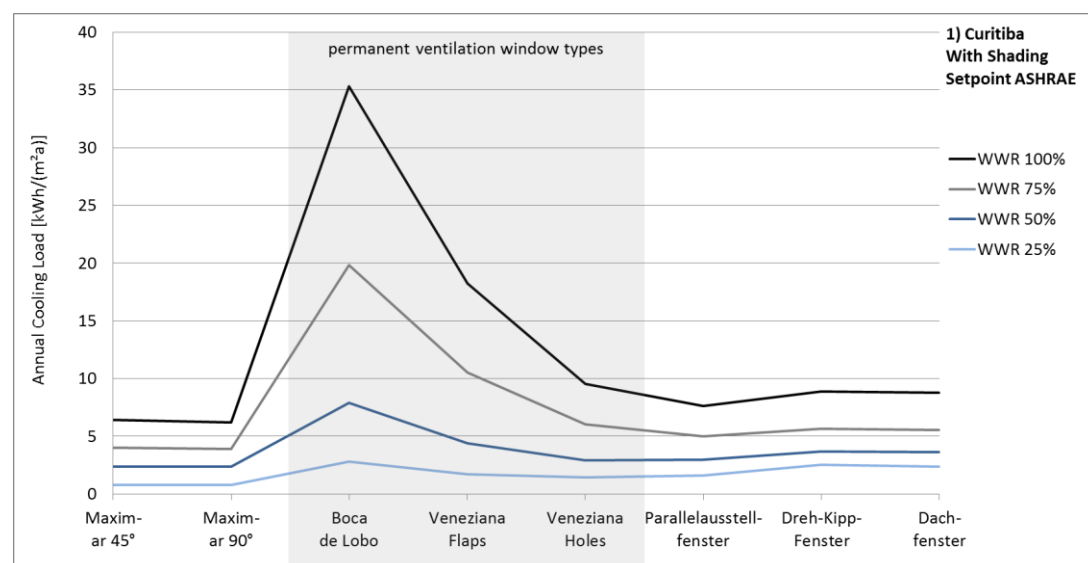


Figure 30: Annual cooling load for the preferred parameters in Curitiba

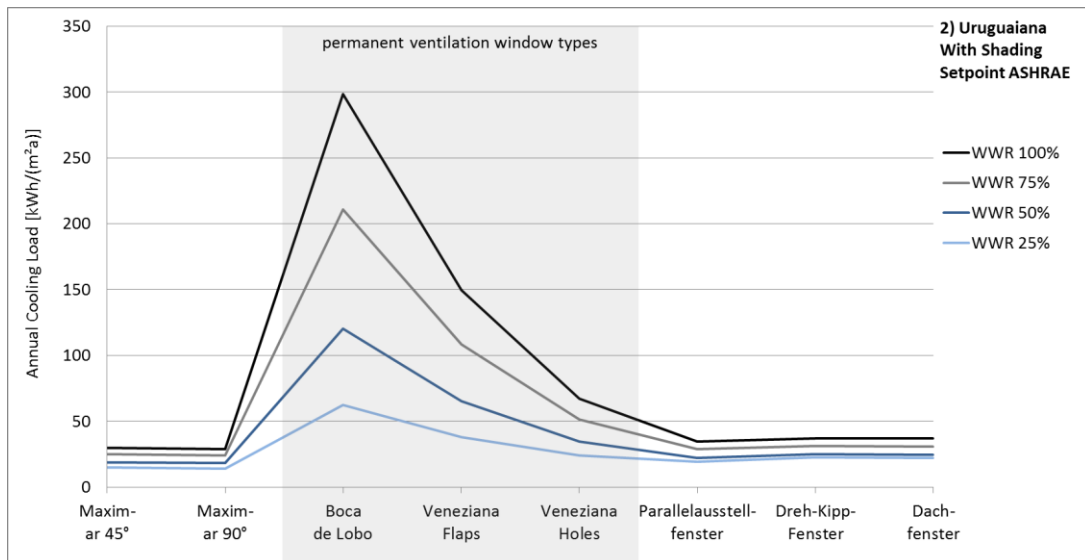


Figure 31: Annual cooling load for the preferred parameters in Uruguaiana

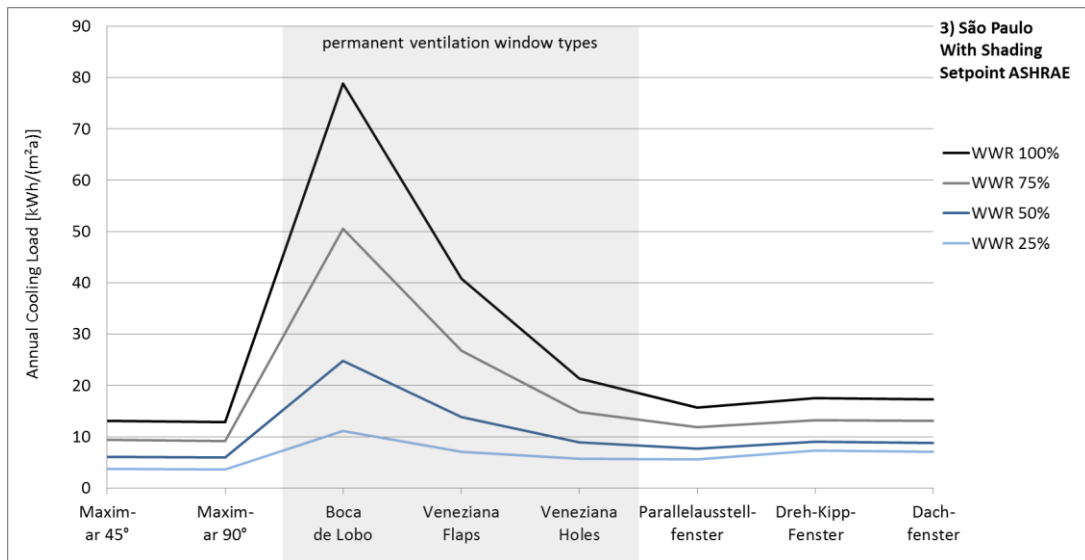


Figure 32: Annual cooling load for the preferred parameters in São Paulo

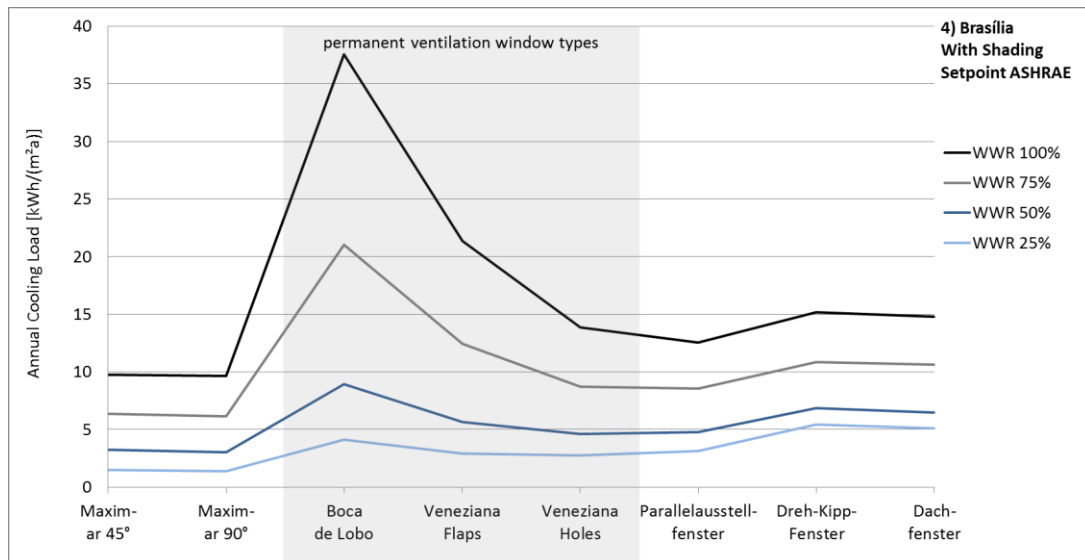


Figure 33: Annual cooling load for the preferred parameters in Brasília

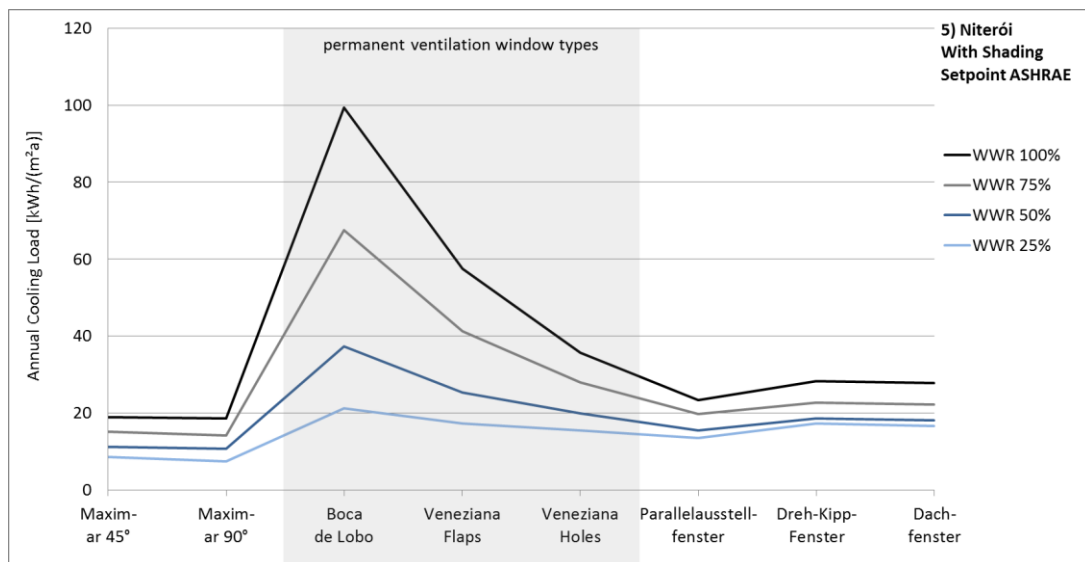


Figure 34: Annual cooling load for the preferred parameters in Niterói

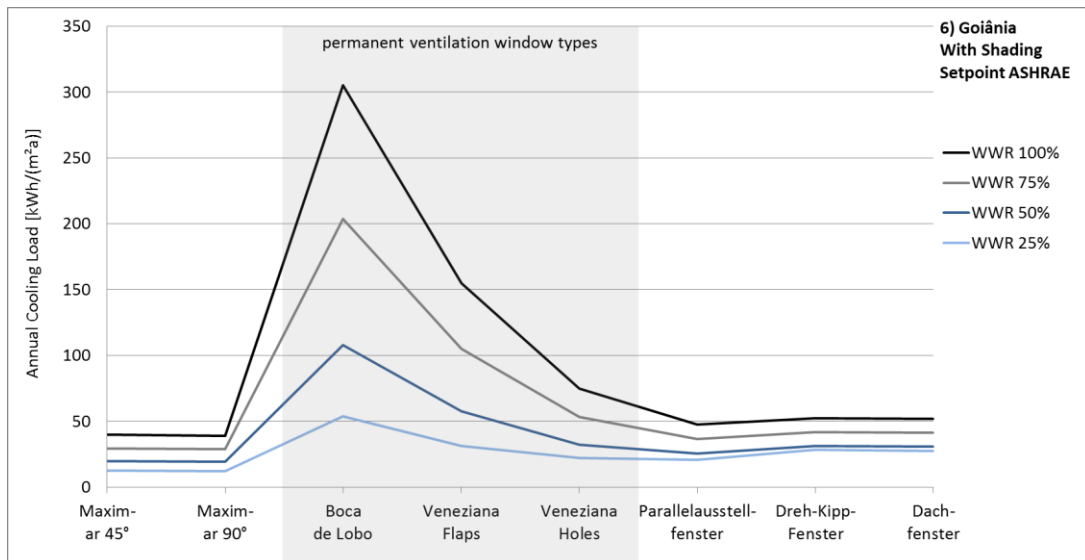


Figure 35: Annual cooling load for the preferred parameters in Goiânia

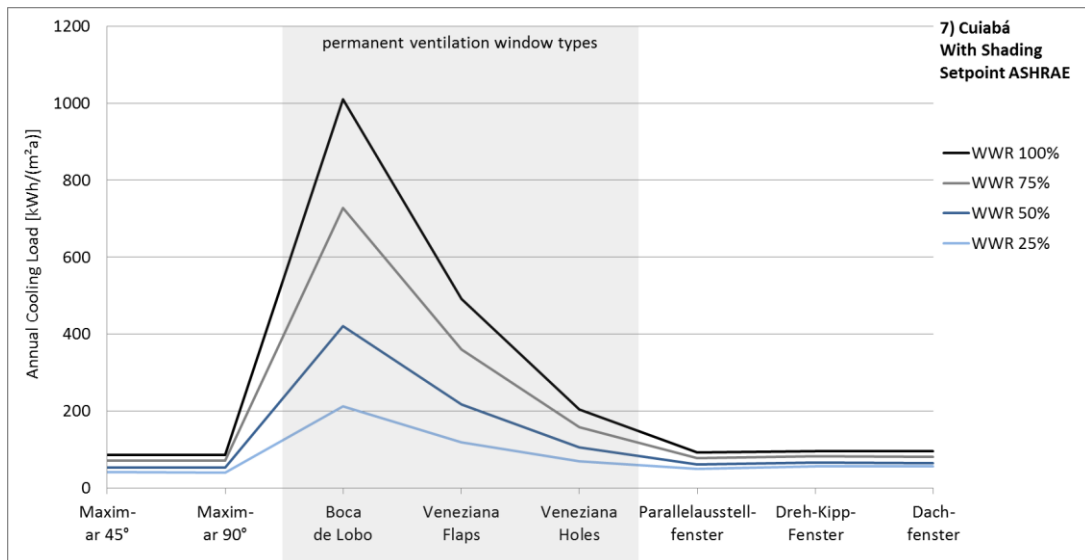


Figure 36: Annual cooling load for the preferred parameters in Cuiabá

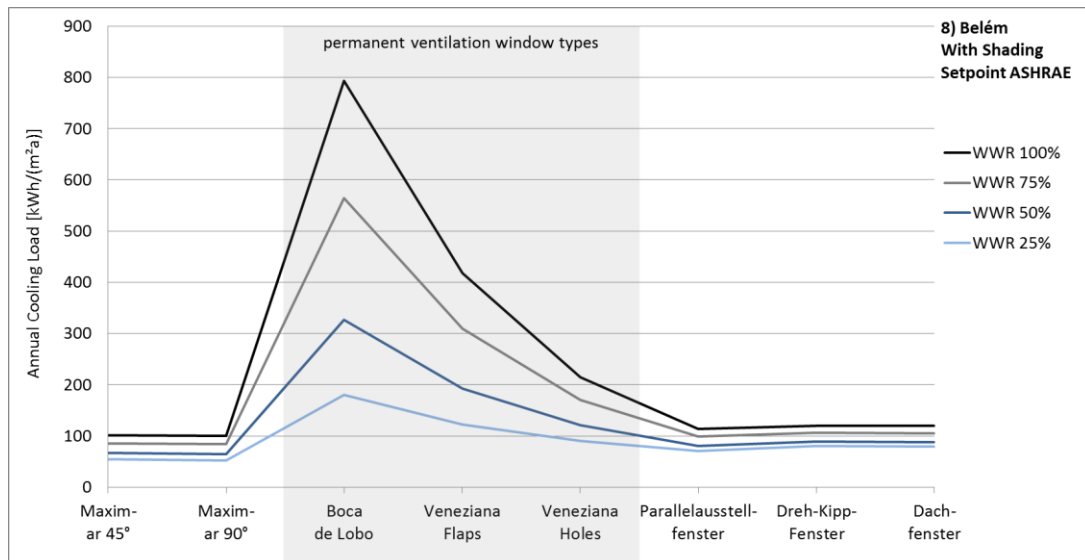


Figure 37: Annual cooling load for the preferred parameters in Belém

4.8 Conclusion

The results show that the energy demand for cooling can be reduced by passive measures. In climates with lower air temperatures (bioclimatic zones 1 and 2) and in climates with noticeable temperature amplitude between day and night (bioclimatic zones 3, 4 and 5) it is not necessary to install air conditioning systems in office buildings if passive measures like intelligent constructions and natural ventilation are used and when the window size is limited. This is expressed by very low energy demand for cooling (less than 10 kWh/(m²a)).

However, the results are subjected to some restrictions. The EnergyPlus simulations are run with statistical weather data for one city representing the whole bioclimatic zone. If local weather data are available, additional individual investigations should be done in order to concretize the results. The office room used for these investigations is based on the study carried out in a building of the Ministry of the Environment and Ministry of Culture, located in Brasília, Brazil. Building components, occupancy as well as the equipment is based on the ministry building. Deviating construction and building use will influence the cooling load. Aiming to improve the energetic performance of buildings by the use of natural ventilation, the current research must be carried out by testing the performance of buildings with different thermal properties for different climates.

Discharge coefficients used in the simulations are determined in wind tunnel experiments. These experiments provide data which are valid for cross ventilation only. All simulations are done with cross ventilation. This method enables much higher airflow rate than single sided ventilation does. This project exposes the potential of natural ventilation in hot climates. With intelligent designed building envelopes and interior tuned to the boundary conditions it is possible to either significantly reduce the energy demand for cooling or to avoid expensive installation and operating of HVAC systems. Knowledge gained in this project shall be used for more detailed analysis in further research.

5 Knowledge Transfer

5.1 SBE16 - International Conference on Sustainable Built Environment (SBE)

The project team attended to the SBE16 - International Conference on Sustainable Built Environment³ from March, 7th to 11th of 2016. A paper written by the project partners about night ventilation in Brazil and Germany was presented at this conference [26]. During the conference week multiple project meetings were done in order to plan the wind tunnel experiments and to contact the German project partner *Lenderoth*.



Figure 38: Project partners at SBE16 in Hamburg

5.2 Training School – Adaptive Facades 2016 (Hamburg, Germany)

The next generation of facades (or building envelopes) consists of multifunctional and highly adaptive systems, where the physical separator between the interior and exterior environment (i.e. the building envelope) is able to change its functional features or behaviour over time in response to transient performance requirements and boundary conditions with the aim of improving the overall building performance. Numerous programs on modern universities are dedicated to the subject of facade design and the number of research groups is steadily increasing. Within the *COST* program in the European Union (Cooperation in Science and Technology), a project *Adaptive Facades Network* was therefore promoted, which offers European scientists a platform to collaborate and exchange perspectives.

To connect the young generation of scientists, a summer school⁴ took place in September 2016 at the *HCU* with a total of 62 participants from 37 universities. In addition to lecturers from Europe, invited experts from Brazil shared their research practices and findings. Their participation was supported by *DAAD*.

³ <http://www.zebau.de/projekte/sbe16-hamburg>

⁴ http://tu1403.eu/?page_id=421

In a very intensive week of lectures and workshops the participating PhD and Master Students had the opportunity to look beyond the scope of their own research and to follow aspects of parallel research on different case studies. Not only new knowledge was gained and shared, but also new long-term cross-border contacts are established to make a prosperous contribution to continuation of the European science-evolving idea.



Figure 39: Participants and Professionals at the 2016 Summer School



Figure 40: Excursion to IBA area in Hamburg visiting the case study houses for energy efficiency



Figure 41: Evaluation of the projects developed during the workshop

5.3 Workshop “Research into Use”

This workshop was part of the project where the research team, partners, representative of the funding agencies and potential partners got together to discuss the results of the research and their application in the market. The aim of this meeting was to identify possibilities to transfer the knowledge gained within the research project to industry, economy, environment and further research.



Figure 42: Brainstorming during the *Research Into Use* workshop

5.4 Training School – Design Process for Building Retrofit 2017 (Campinas, Brazil)

The Training School 2017 was organized by the School of Civil Engineering, Architecture and Urban Design at *Unicamp*, Brazil. It was addressed to Master and PhD students from Brazil and Germany. In the first part of the event, lectures on *Design Process for Building Retrofit* were presented by Brazilian and German experts in the field of building design and retrofit process. In the second part, which was based on the input given during the lectures and their backgrounds, the participants were divided in teams. These teams created conceptually retrofit studies for a given case of institutional building in Brazil, guided by experts from Germany and Brazil. With the results of the workshop, the students prepared a final analysis of their conceptual design.



Figure 43: Participants and Professionals at the 2017 Summer School



Figure 44: Workshop phase during the 2017 Summer School

6 Acknowledgements

The authors would like to acknowledge DAAD and CAPES for funding this research, GIZ for the support, the companies Christophe Lenderoth GmbH and MGM for providing window samples to be tested in the wind tunnel. Thanks to Edson Matsumoto and Prof. Paulo Vatauvuk for their help on understanding and operating the wind tunnel, to Daniel Cóstola for his valuable contributions during the project and Felipe da Silva Duarte Lopes and Juliane Fritz Benachio for helping with the setup of the experiments.

Literature

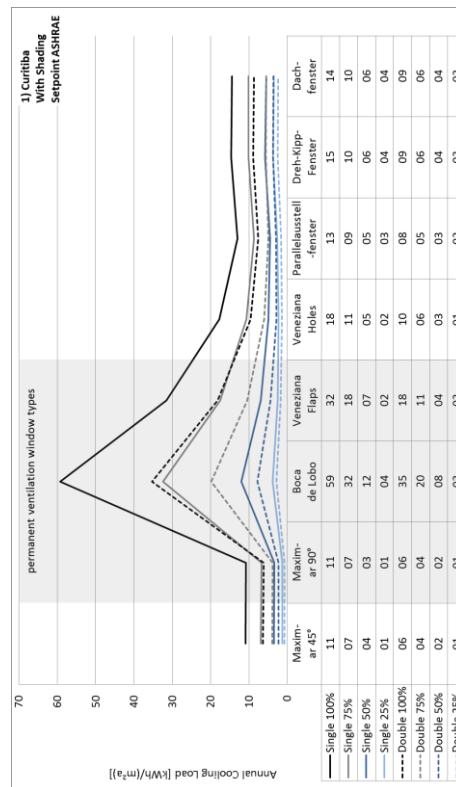
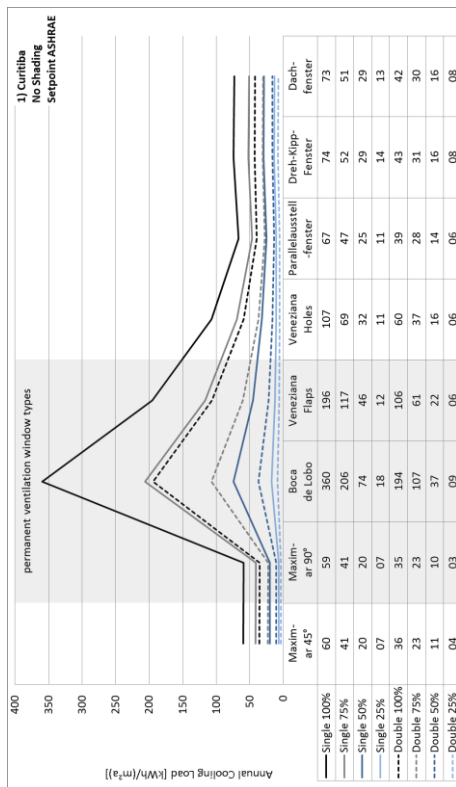
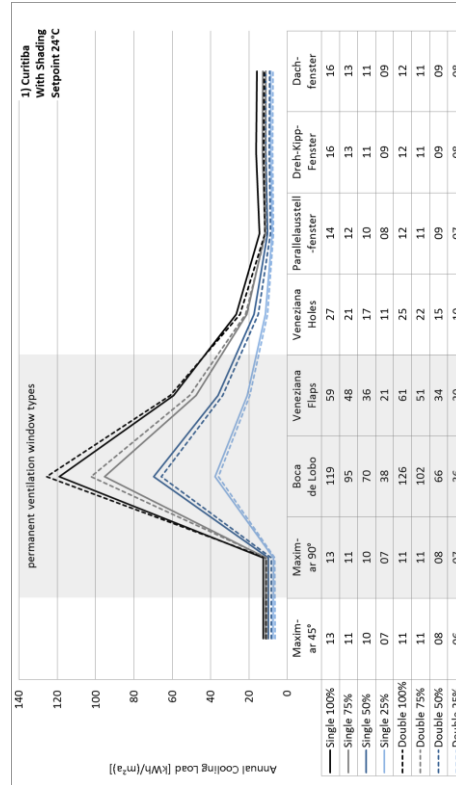
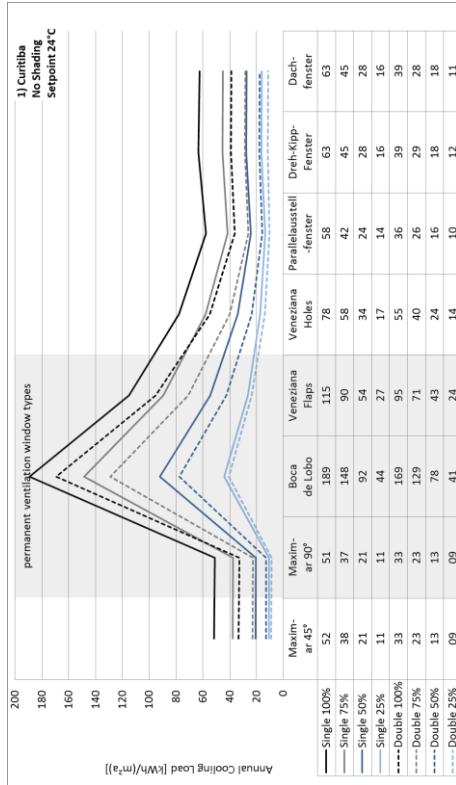
- [1] P. Karava, T. Stathopoulos and A. K. Athienitis, "Wind Driven Flow through Openings - A Review of Discharge Coefficients". *International Journal of Ventilation* 3(3), 2004.
- [2] J. Wang, S. Wang, T. Zhang and F. Battaglia, "Assessment of single-sided natural ventilation driven by buoyancy forces through variable window configurations," *Energy and Buildings* (139), pp. 762-779, 2017.
- [3] Q. Chen, "Ventilation performance prediction for buildings: A method overview and recent applications," *Building and Environment*, vol. 44, pp. 848-858, 2009.
- [4] *BS EN 13141-1:2004 Ventilation for buildings - Performance testing of components/products for residential ventilation - Part 1: Externally and internally mounted air transfer devices.*
- [5] C. R. Chu, Y. -H. Chiu, Y. -J. Chen, Y. -W. Wang and C. -P. Chou, "Turbulence effects on the discharge coefficient and mean flow rate of wind-driven cross-ventilation," *Building and Environment*, vol. 44, pp. 2064-2072, 2009.
- [6] Y. H. Chiu and D. W. Etheridge, "External flow effects on the discharge coefficients of two types of ventilation opening," *Journal of Wind Engineering and Industrial Aerodynamics* vol. 95, pp. 225-252, 2007.
- [7] I. Idelchick, *Handbook of Hydraulic Resistance* (3rd Edition), Jaico Publishing House, 2001.
- [8] M. Ohba, K. Irie and T. Kurabuchi, "Study on airflow characteristics inside and outside a cross-ventilation model, and ventilation flow rates using wind tunnel experiments," *Journal of Wind Engineering and Industrial Aerodynamics* 89(2001), pp. 1513-1524.
- [9] M. Ohba, T. Kurabuchi, T. Endo, Y. Akamine, M. Kamata and A. Kurahashi, "Local dynamic similarity model of cross ventilation, Part 2, Application of local dynamic similarity model," *International Journal of Ventilation*, pp. 383-393, 2004.
- [10] T. Sawachi, "Detailed observation of cross ventilation and air flow through large openings by full scale building model in wind tunnel," *Proceedings of Rovent, Copenhagen, Denmark*, pp. 565-568, 2002.
- [11] B. J. Vickery and C. Karakatsanis, "External wind pressure distributions and induced internal ventilation flow in low-rise industrial and domestic structures," *ASHRAE Transactions* (93-2), pp. 2198-2213, 1987.

- [12] A. Maas, "Experimentelle Quantifizierung des Luftwechsels bei Fensterlüftung," Kassel (DE), 1995.
- [13] Verein Deutscher Ingenieure, "VDI 4300 Part 7 - Indoor air pollution measurement. measurement of the indoor air change rate," July 2007.
- [14] Umweltbundesamt [German Environment Agency], "Gesundheitliche Bewertung von Kohlendioxid in der Innenraumluft," *Bundesgesundheitsbl - Gesundheitsforsch - Gesundheitsschutz*, pp. 1358-1369, 2008 - 51.
- [15] D. Laussmann and D. Helm, "Air Change Measurements Using Tracer Gas," Robert Koch Institute, Germany.
- [16] H.-D. Schulze and G. Schuschke, "Studie über Notwendigkeit und Zuverlässigkeit von Luftwechsel und Luftvolumenstrommessungen," *Gesundheits-Ingenieur Haustechnik Bauphysik Umwelttechnik*, pp. 12-16, 111 (1990) Heft 1.
- [17] W. Raatschen, "Tracergasmessungen in der Gebäudetechnik," *Gesundheits-Ingenieur Haustechnik Bauphysik Umwelttechnik*, pp. 78-87 & 129-138, 116 (1995) Heft 2 & 3.
- [18] F.-D. Heidt and H. Werner, "Microcomputer-aided measurement of air change rates," *Energy and Buildings*, pp. 313-320, Vol. 9, No. 4 (December 1986).
- [19] "ASHRAE Handbook Fundamentals," 2004.
- [20] T. S. Larsen, "Natural Ventilation Driven by Wind and Temperature Difference," Aalborg University, Department of Civil Engineering, Aalborg, 2006.
- [21] O. K. Larsen, "Double-Skin Facade," Aalborg University, Department of Civil Engineering, Aalborg, 2008.
- [22] BRASIL - Ministério do Meio Ambiente, "Memorial de simulação e relatório das propriedades térmicas," 2015.
- [23] R. Judkoff and J. Neymark, "International Energy Agency building energy simulation test (BESTEST) and diagnostic method," Golden, 1995.
- [24] ABNT - Associação Brasileira de Normas Técnicas, "Projeto 02:135.07-001/3, Desempenho térmico de edificações Parte 3: Zoneamento bioclimático brasileiro e diretrizes construtivas para habitações unifamiliares de interesse social," 2003.
- [25] A. Walsh, D. Cóstola and L. C. Labaki, "Review of methods for climatic zoning for building energy efficiency programs," *Building and Environment (Vol. 112)*, pp. 337-350, 2017.

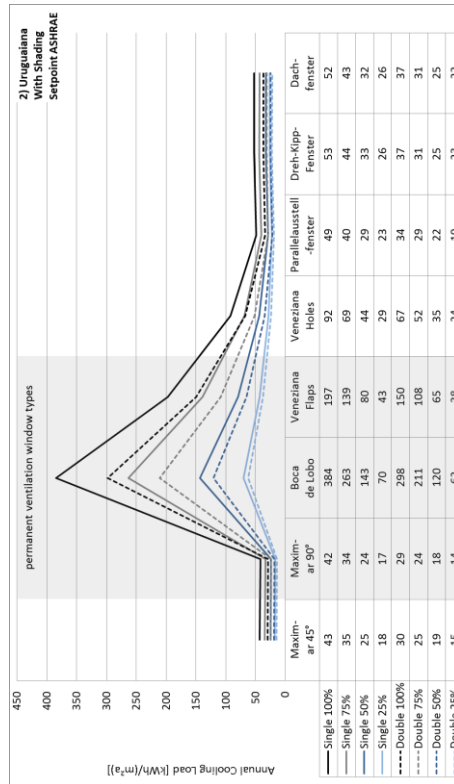
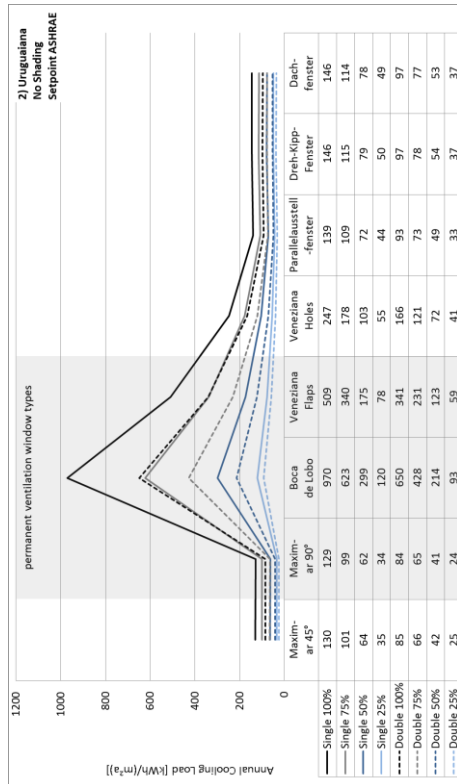
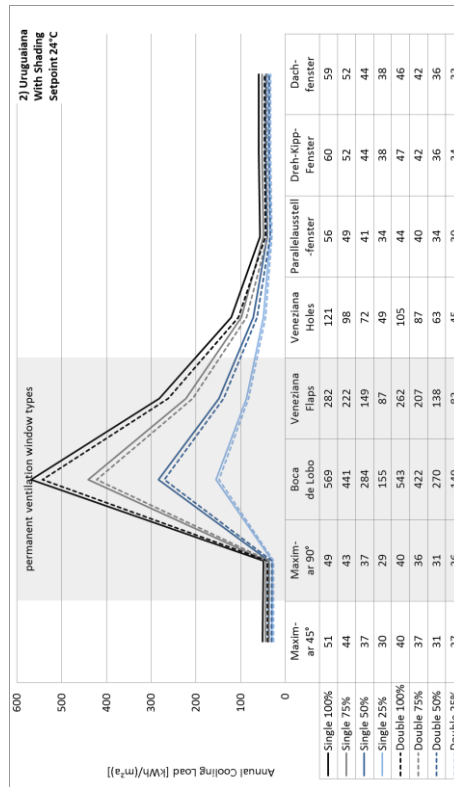
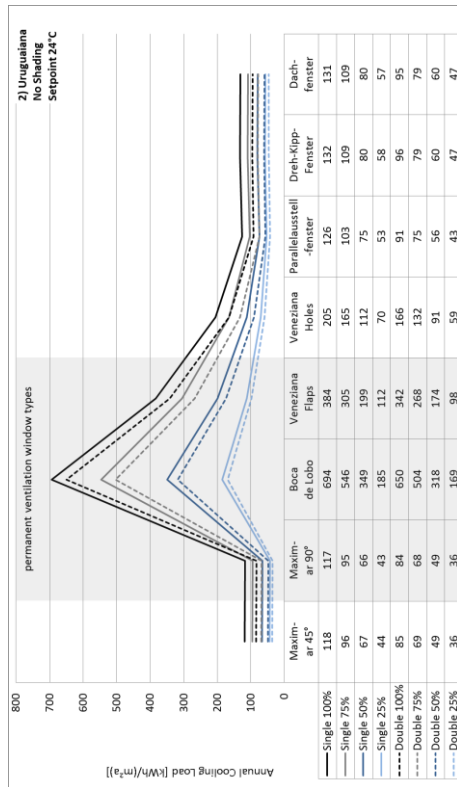
- [26] F. Wellershoff, M. Friedrich, L. C. Labaki and L. Fernandes, "Façade design for night cooling by natural ventilation in different climate zones," *Conference Proceedings - Sustainable Built Environment Conference 2016 in Hamburg : Strategies, Stakeholders, Success factors*, pp. 572-581, 2016.
- [27] Y. -H. Chiu and D. W. Etheridge, "External flow effects on the discharge coefficients of two types of ventilation opening," *Journal of Wind Engineering and Industrial Aerodynamics*, vol. 95, pp. 225-252, 2007.
- [28] R. Lamberts, L. Dutra and F. O. R. Pereira, "Eficiência Energética na Arquitetura (3a Edição)," 2014.
- [29] C. R. Chu, Y. H. Chiu, Y. J. Chen, Y. W. Wang and C. P. Chou, "Turbulence effects on the discharge coefficient and mean flow rate of wind-driven cross-ventilation," *Building and Environment vol 44*, pp. 2064-2072, 2009.

Appendix

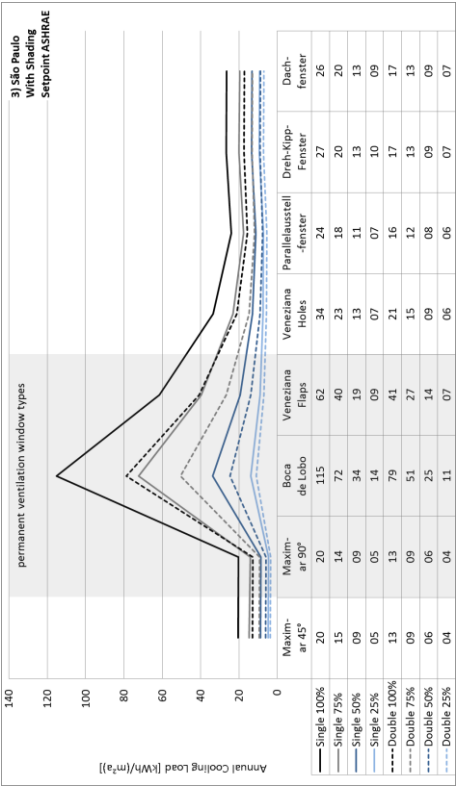
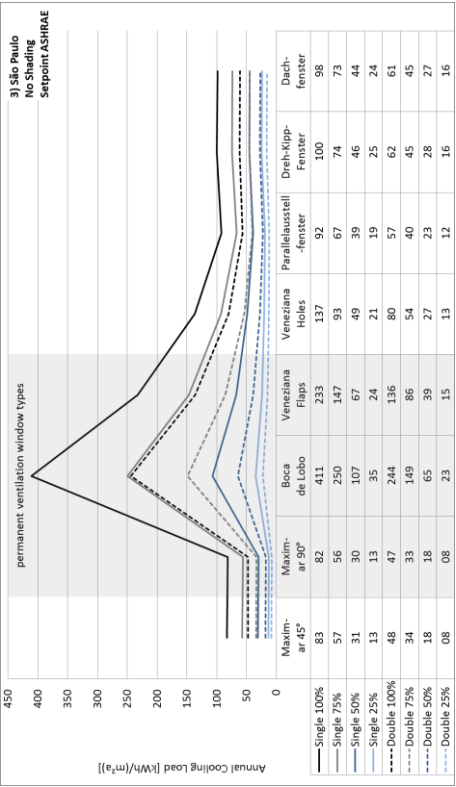
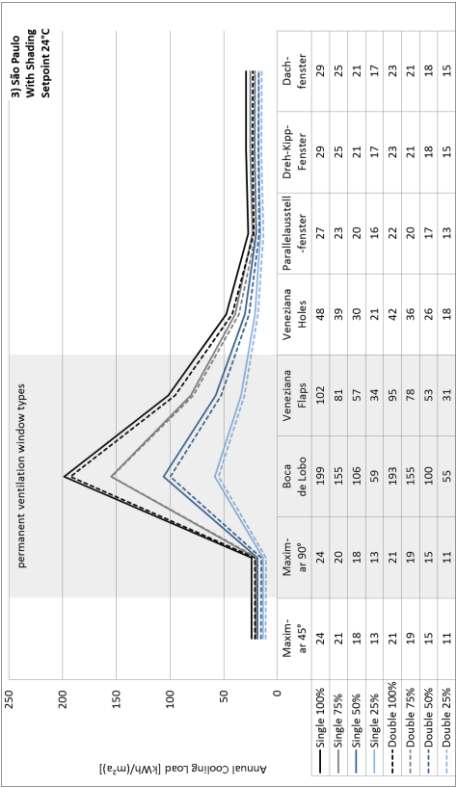
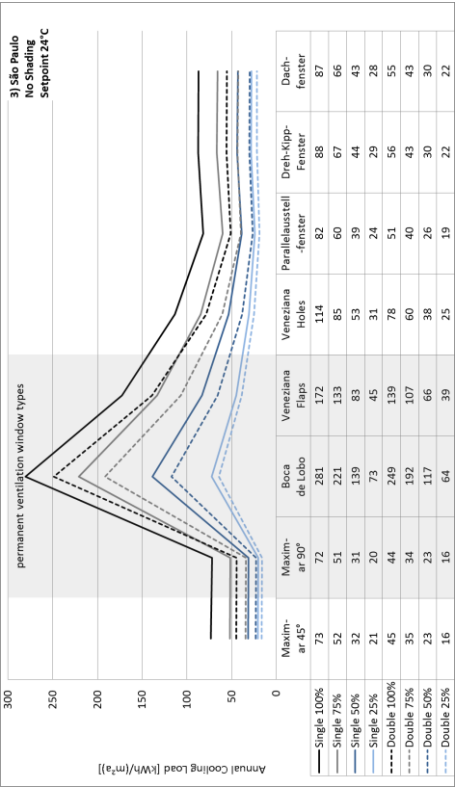
Climate 1: Curitiba



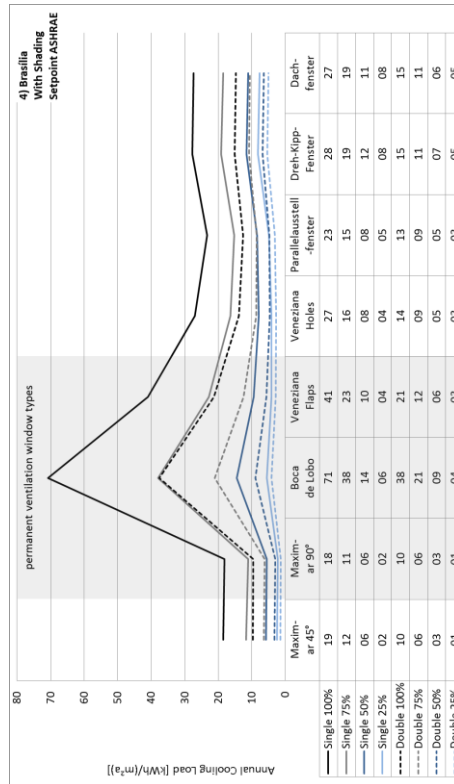
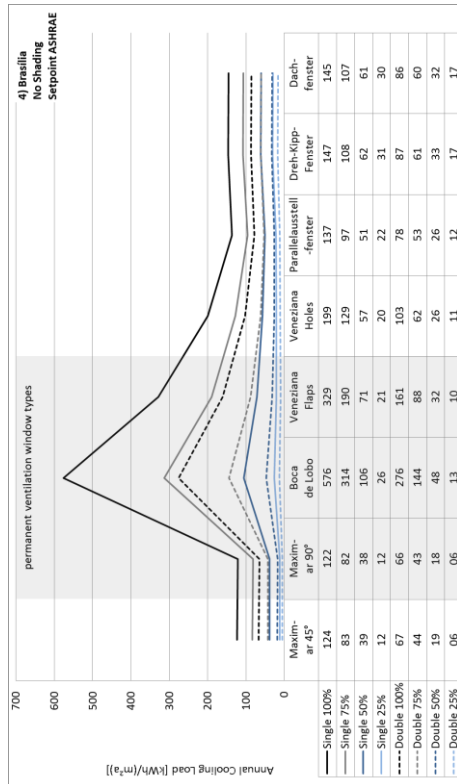
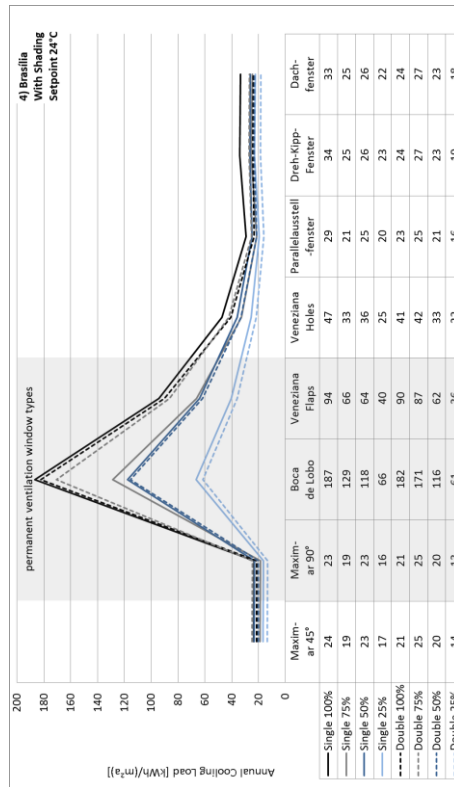
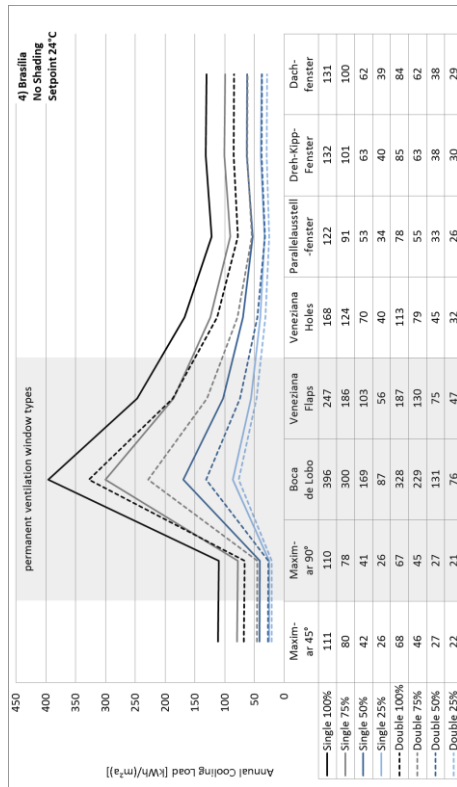
Climate 2: Uruguaiiana



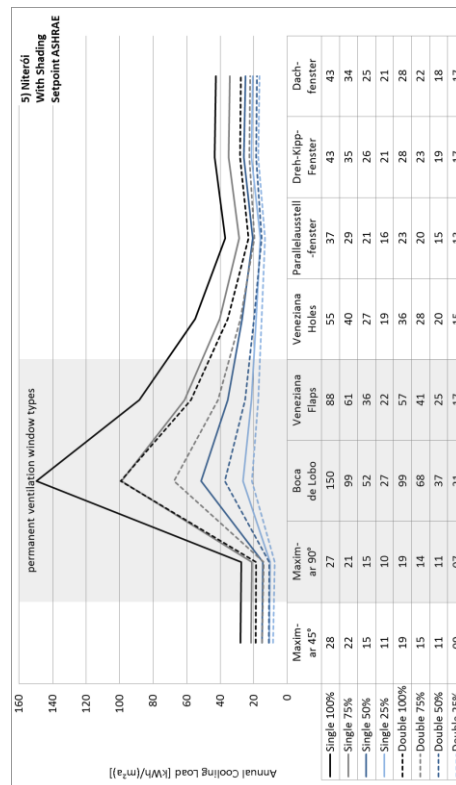
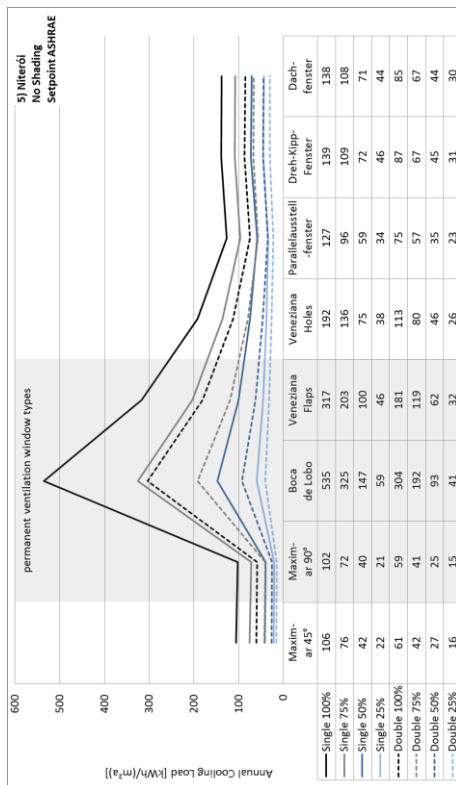
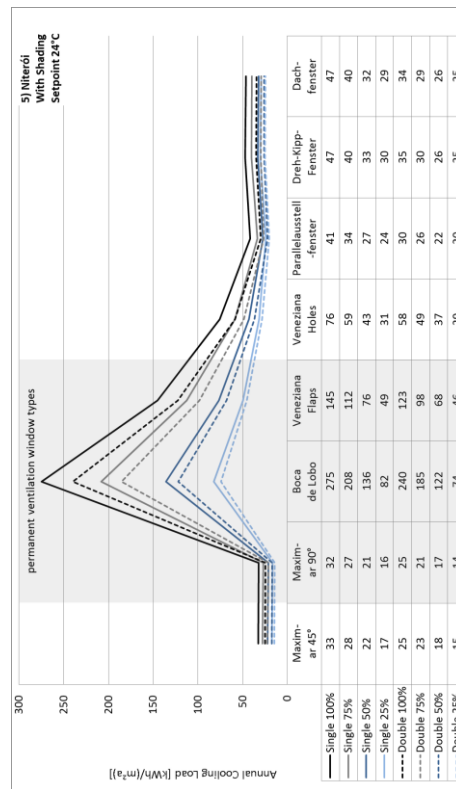
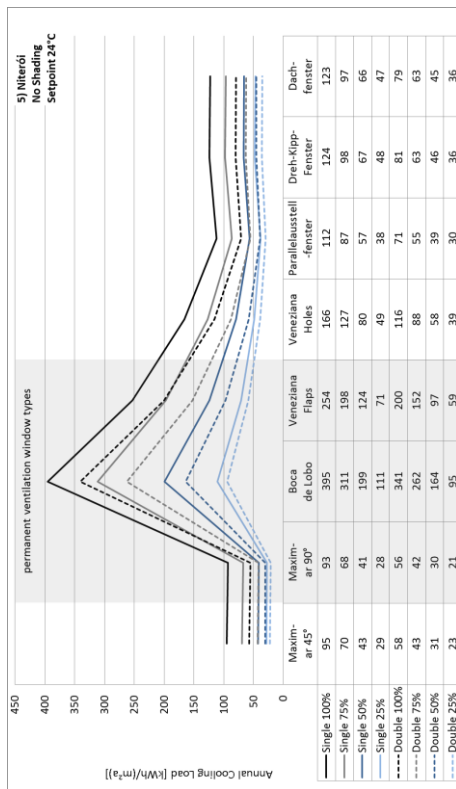
Climate 3: São Paulo



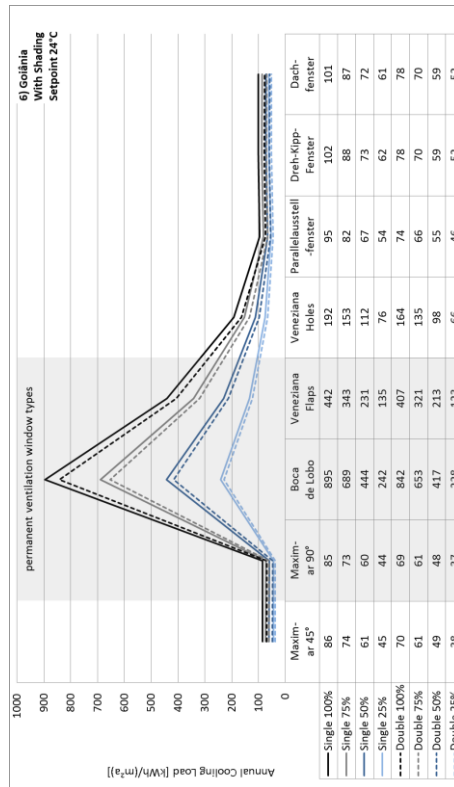
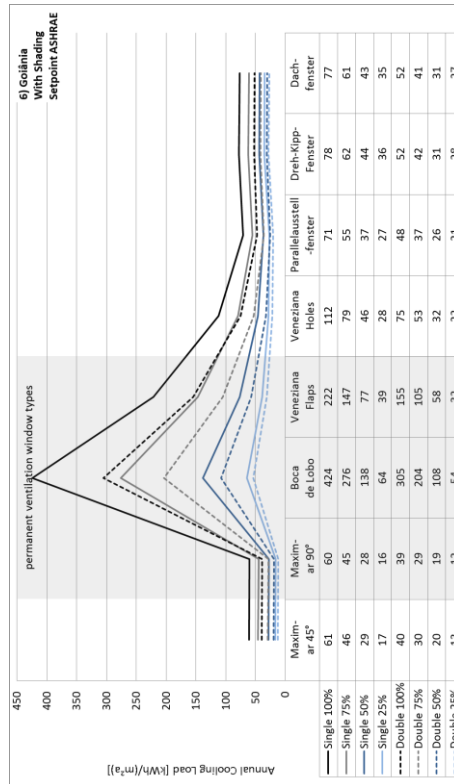
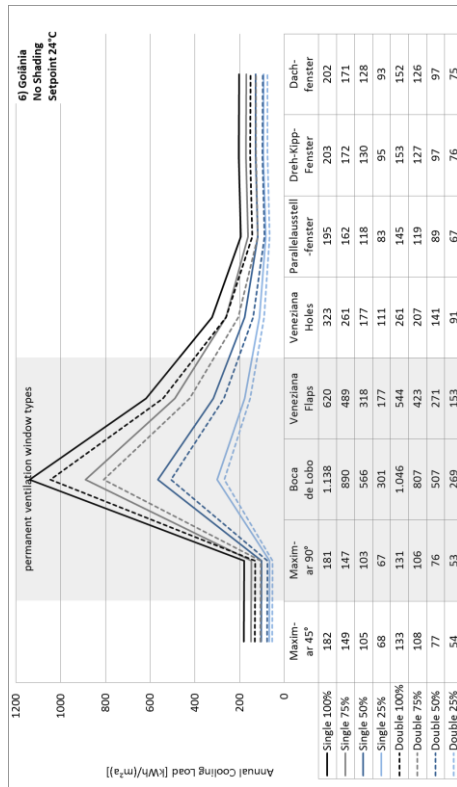
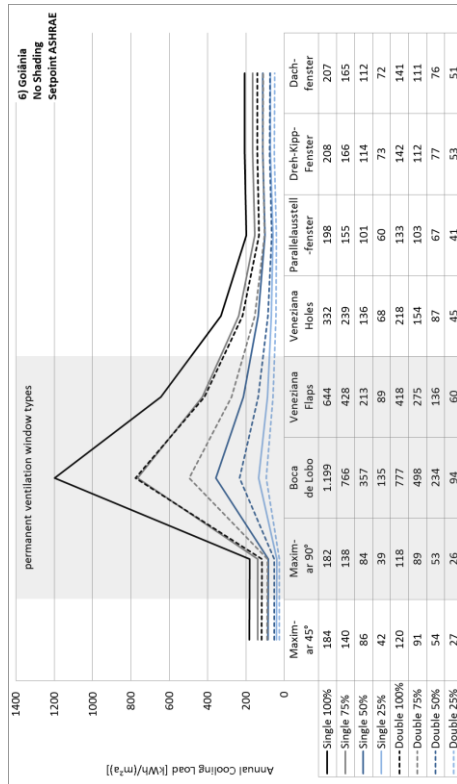
Climate 4: Brasília



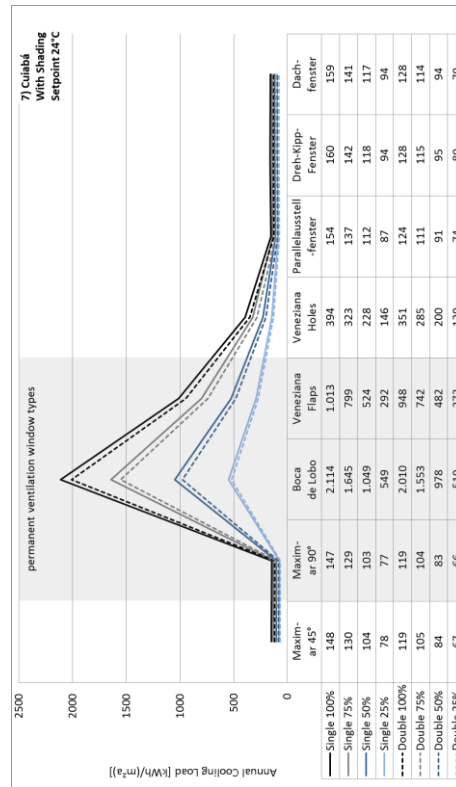
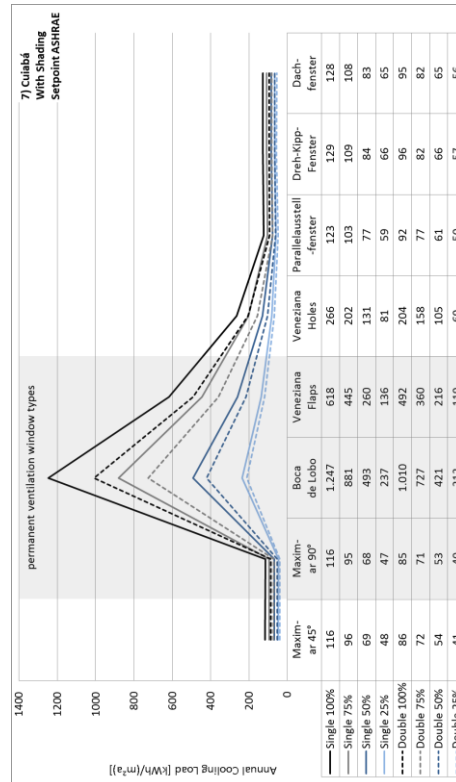
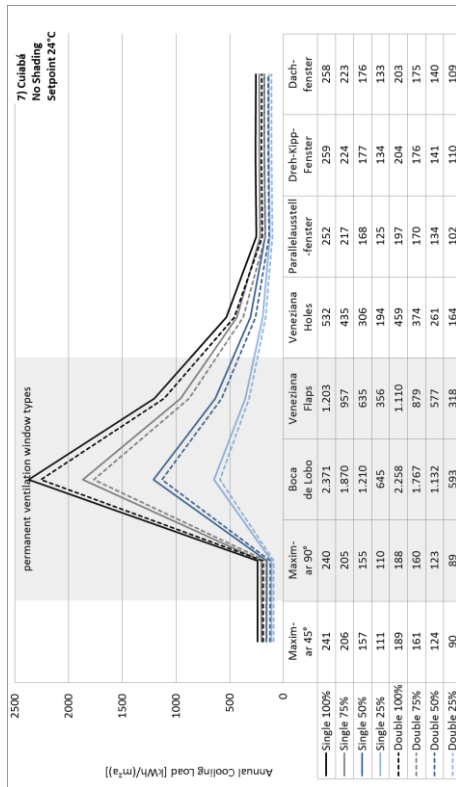
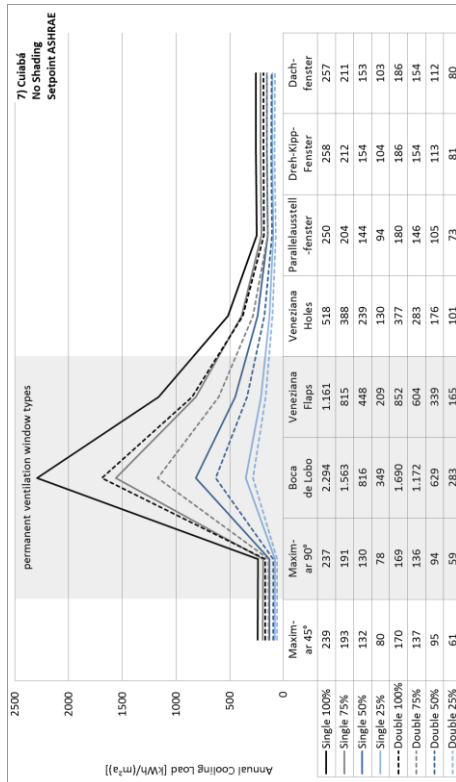
Climate 5: Niterói



Climate 6: Goiânia



Climate 7: Cuiabá



Climate 8: Belém

